Journal of CO2 Utilization 47 (2021) 101475

Contents lists available at ScienceDirect

Journal of CO2 Utilization

journal homepage: www.elsevier.com/locate/jcou

Immobilization of carbonic anhydrase for CO_2 capture and its industrial implementation: A review

Cristhian Molina-Fernández [a,b], Patricia Luis [a,b,*]

[a] Materials & Process Engineering (iMMC-IMAP), UCLouvain, Place Sainte Barbe 2, 1348 Louvain-la-Neuve, Belgium
[b] Research & Innovation Centre for Process Engineering (ReCIPE), Place Sainte Barbe, 2 bte L5.02.02 – B, 1348 Louvain-la-Neuve, Belgium

ARTICLE INFO

Keywords:
Carbonic anhydrase
CO_2
Immobilization

ABSTRACT

Minimal cost per ton of captured CO_2 and associated environmental impacts are considerable barriers for the industrial implementation of post-combustion CO_2 capture. Aqueous solvents promoted with the enzyme carbonic anhydrase are a promising alternative to replace energy intensive and environmentally unfriendly amine-based solutions, which are currently benchmark solvents in CO_2 absorption. However, using free enzyme in solution requires significant amounts of enzyme in addition to its possible denaturalization. Enzyme immobilization appears as a rational approach to develop a novel CO_2 capture system using aqueous solvents. In the recent literature, efforts are focused on the development and characterization of different carriers and immobilization strategies to achieve good activity and stability compared to free enzyme in solution. In the laboratory and the industry, immobilized carbonic anhydrase have been already tested in a variety of configurations including packed columns, gas-liquid membrane contactors, dynamic devices and selective membranes. This article reviews the developments, opportunities and limitations found at laboratory scale as well as in the industry, and brings them together in order to identify the key challenges and perspectives in the industrial implementation of immobilized carbonic anhydrase for CO_2 capture.

1. Introduction

Global warming is a major concern. The alarming increase of atmospheric CO_2 levels is fostering the research community and the industry to look for solutions to stop the steady increase of global temperature and its drastic consequences. Our high and continuously increase of energy demand and our reliance in a fossil fuel energy stock makes this problem a huge challenge [1]. A significant amount (more than 40%) of global greenhouse emissions are caused by the energy industry, mainly heat and power generation [2]. Emissions from this sector are gases generated by combustion of fossil fuels, the so-called flue gases. Because they are localized point emissions compared to other major contributors to global warming such as transport, the application of CO_2 capture strategies becomes a tentative choice. Two main alternatives are possible after the CO_2 has been captured: geological storage or utilization [3]. Regardless the final use of CO_2, post-combustion CO_2 capture is a difficult task considering that CO_2 is a stable molecule [4], it has a low partial pressure (10–20%), the flue gas has high temperature (100−250 °C) and CO_2 is accompanied by other compounds (H_2O, NO_X, SO_X, etc.) [5,6]. For CO_2 separation, chemical absorption using amines is the most popular separation technology due to is high efficiency, low cost and maturity [7,8] (Fig. 1a). However, it has been indicated that chemical absorption with amines, although technically feasible, does not represent an attractive solution for CO_2 separation from flue gases in a global scale [9]. In addition to the CO_2 emissions related to the production process of the amines, several drawbacks in the use of amines as absorption solvent can be pointed out: high toxicity, corrosively, degradability, high volatility [8,10–12] (Fig. 1b) and the large energy required to regenerate the solvent and to recover the CO_2 [13]. Despite of these disadvantages, most reported cases of post-combustion CO_2 capture are using amine absorption [14].

Other solvents than amines have also been suggested, such as aqueous solutions of Na_2CO_3, K_2CO_3, ammonia, amino acids, etc [13]. Although requiring less energy for regeneration [13], they are generally limited by the low reaction rate of CO_2 in the liquid phase. This is due to the slow CO_2 hydration kinetics [15]. One of the current trends to solve this issue is the use of carbonic anhydrase because it catalyzes the reversible hydration reaction of CO_2.

Carbonic anhydrase (CA) is an ancient metalloenzyme ubiquitous in Nature [16]. In fact, it is one of the most actives enzymes with a turnover

* Corresponding author at: Materials & Process Engineering (iMMC-IMAP), UCLouvain, Place Sainte Barbe 2, 1348 Louvain-la-Neuve, Belgium.
E-mail address: patricia.luis@uclouvain.be (P. Luis).

https://doi.org/10.1016/j.jcou.2021.101475
Received 15 December 2020; Received in revised form 5 February 2021; Accepted 8 February 2021
Available online 5 March 2021

number up to 10^6 s^{-1} [17]. Several types of CA are available, each characterized by different structure and properties [18,19]. Although most of the studies discussed in this review have been focused on CA from bovine erythrocytes, the use of CA from thermophilic organisms is particularly interesting considered its resistance to high temperatures [20,21]. Because its high activity, CA promoted aqueous solvents show significant improvements in CO_2 absorption rate as this enzyme catalyzes the rate limiting step that is CO_2 hydration [15,22–25]. There some CO_2 capture industrial projects involving CA to activate a variety of solvents (see the review by Sharma et al. [19]). However, it is a well-known fact that working with free enzymes in solution has a number of disadvantages. Enzyme are "fragile" molecules with a limited range of working conditions (temperature, pH and ionic strength). Their small size (the average size of CA is $5 \times 4 \times 4$ nm^3 [17]) makes them difficult to recover and recycle [26,27]. In CO_2 capture via absorption, CA would be dissolved in the solvent. Therefore, in the case of subsequent thermal desorption of CO_2 (see Fig. 1a), the temperatures required in the stripper could denaturalize the enzyme [28]. If instead, CO_2 is recovered in the form of carbonate/bicarbonate crystals, after the saturated solvent is sent to a crystallization unit, high ionic strength and pH could also lead to enzyme deactivation [28]. As a consequence, in industry enzymes are very often immobilized [29,30]. Immobilization improves enzyme recovery and reusability decreasing enzyme overall cost. It can also make the enzymes more stable through protection from the media or via protein structure stabilization. In many situations, immobilization leads to an apparent activity reduction due to a number of factors: mass transfer limitations, enzyme conformation alteration (likely reduction in enzyme turnover), partitioning of substrate and products in the carrier or different enzyme catalysis in the local microenvironment [27,31,32]. Many procedures of immobilization are possible each of them with their strengths and weaknesses [33].

In this review, the different methods that have been reported up to now to immobilize CA are described, giving special attention to the type of immobilization and kind of materials and including a discussion in terms of activity, stability, reusability and enzyme loading. The free-enzyme state is used as reference. Additionally, the different technologies to capture CO_2 taking advantage of immobilized CA will be examined, addressing the theory behind, the existing configurations, key scientific literature (modelling and experimental work) and patents. Finally, conclusions will be drawn bringing both parts of the review together and highlighting challenges and future perspectives.

2. Immobilization strategies of carbonic anhydrase

As indicated previously, enzyme immobilization is a classical methodology to increase enzyme stability and reusability. A large variety of immobilization methods are possible, some based on a single immobilization principle i.e. covalent bonding, adsorption, cross-linked enzyme aggregates, encapsulation or entrapment, while others are a combination of them (Fig. 2). In this section, an overview of the different immobilization materials and methods is disclosed. Table 1 presents a detailed comparison in terms of activity, thermal and storage stability, reusability and enzyme loading.

2.1. Adsorption

Weak forces mediated enzyme-support attachment is a simple immobilization method. Weak interactions such as hydrogen bonds, electrostatic, hydrophobic or Van der Waals forces between enzyme and material surface allow enzyme immobilization simply by incubation under certain (optimized) conditions. In order to attain maximal activity, immobilization optimization generally involves studying the effect of enzyme concentration in the incubation solution, material dose, temperature, incubation time, pH and agitation speed (see references in this section). Low enzyme loading will not fully exploit the carried but too high loading can be detrimental as well due to enzyme crowding and enzyme multilayering [34]. Mild interactions with the support ensures in many cases small conformational changes upon immobilization [30,35,36]. This depends strongly on the nature of the support. Hydrophilic supports tend to be more suitable for adsorption than hydrophobic ones [32,34]. In porous materials, conformational changes could more important in supports with a pore size close to CA dimensions [35]. Yet these weak interactions can limit conformational mobility increasing immobilized enzyme stability compared to free enzyme [37,38]. In the quest for best performance, inorganic materials, (bio)polymers and composite materials have been studied. With regards to the first type, most of the studies have used porous silica as support [35,36,39,40]. Shao et al. [35] immobilized CA into mesoporous molecular sieves with the same chemical composition but different structure (1D, 2D and 3D) and pore sizes. Therefore, CA was immobilized within the pore or/and at the material surface deeding on pore size. For the former case, higher enzyme stabilization is achieved but the efficiency is lower because protein conformational alteration. Similarly, Wanjari et al. [39] focused on mesoporous aluminosilicates and Vinoba et al. [40] studied spherical

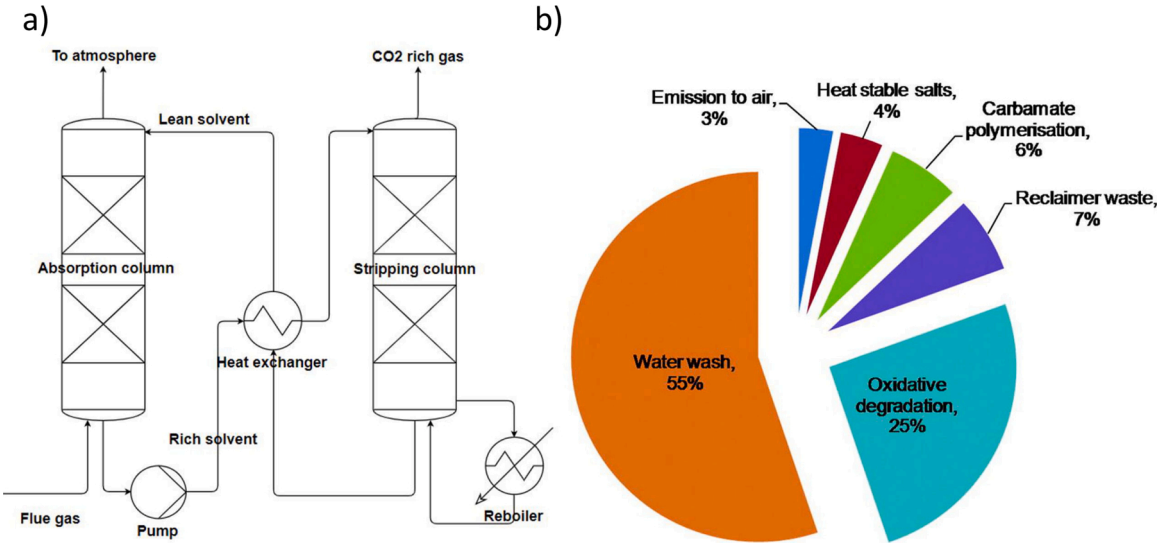

Fig. 1. (a) typical absorption-desorption system; (b) processes that cause MEA losses. Water wash refers to the recovery of evaporated solvent in the CO_2 rich gas via absorption with water. Fig. 1b reprinted with permission from [12]. Copyright (2012) American Chemical Society.

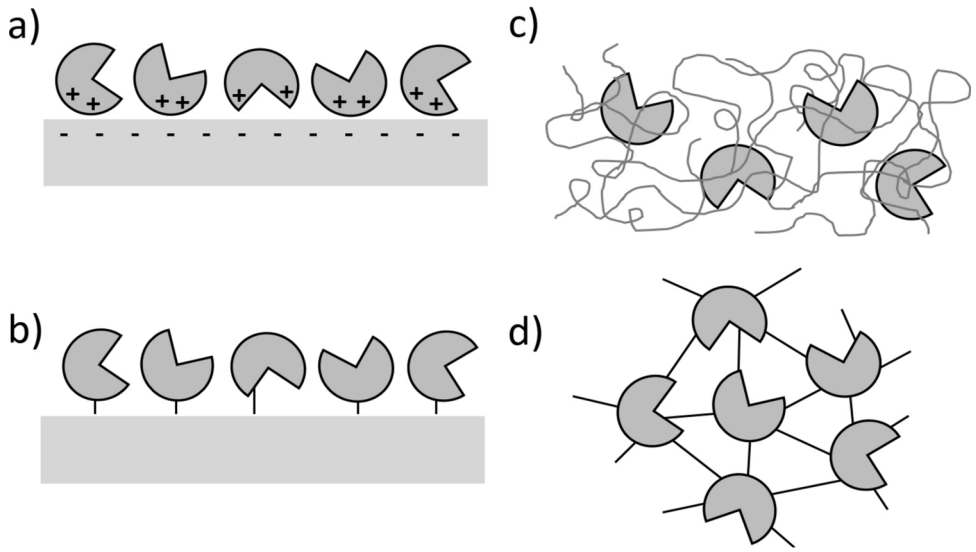

Fig. 2. Traditional immobilization methods: (a) adsorption, (b) surface covalent attachment, (c) entrapment within a polymer and (d) cross-linked enzyme aggregates.

SBA-15 (mesoporous silica). Their studies concluded that there is an important activity reduction during reutilization. Since CA is immobilized by weak forces, the enzyme desorbs eventually decreasing carrier apparent activity. In contrast, in a later publication, Vinoba et al. studied SBA-15 covered by silver [41] or gold [42] nanoparticles in which CA was adsorbed by electrostatic interaction. Here, they obtained a much better reusability, especially in gold nanoparticles, due to the large strength of protein-metal interaction. CA immobilization in silica is through interaction with its hydroxylated surface (silanol groups) [43]. As nanoparticles present large specific surface, enzyme loading was remarkably high. In any case, once exhausted, carriers can be reloaded by placing them in contact with fresh CA solution. It is important to consider that enzyme adsorption is a nonspecific process. If the CA solution contains other proteins it can have a detrimental effect. To solve this issue, Kim et al. [37] modified CA with an appropriate peptide in order to selectively adsorb this protein on inorganic carriers: silica and titania particles. Under optimized conditions recombinant CA was selectivity immobilized with respect to other proteins present in crude cell lysates allowing direct immobilization without previous CA purification. Here again, these immobilized biocatalysts had a better reusability. Concerning biopolymers, Hou et al. [21] studied chitin. In order to achieve direct enzyme binding to chitin, the protein was genetically modified to incorporate a chitin-binding domain. Promisingly, the best results in terms of activity were obtained when using raw chitin. In another example, Hosseinkhani et al. [44] immobilized CA (fresh and partially denaturalized) on to hydrophobic adsorbents, i.e. Sepharose-lipid (octyl, dodecyl and palmityl). Not only partially denatured enzyme is able to interact with the hydrophobic carried while fresh is not but also adsorption of partially denatured enzyme avoids its irreversible denaturation. Despite of these examples, chitosan (a chitin derivate) has received the major attention to form biopolymers and composite materials for CA immobilization by adsorption [38,45–48]. This hydrophilic biopolymer presents electropositive charge and several functional groups with which CA can form hydrogen bonds [49]. Chitosan usage as CA immobilization matrix includes chitosan beads prepared through different procedures [45–47], chitosan-alginate beads [46,47], chitosan composites with poly(vinyl alcohol), clay and mesoporous alumina [46] and chitosan stabilized iron nanoparticles [38]. Each of them providing different results. Whereas most of them (and most of the studies discussed in this review) have been focused on immobilizing the enzyme, Pranhu et al. [46] and Sharma et al. [47] immobilized whole cell CA enriched organisms. Different activities where observed when immobilizing CA and a CA enriched organisms in the same chitosan based material. They also found that the efficiencies were generally lower for whole cell immobilization compared to purified CA. The same authors studied the popular biopolymer alginate as carrier. However, CA loading and efficiency were lower than for chitosan based carriers. Regarding other composite supports, biopolymer templated mesoporous alumina has also been investigated as support for CA. So far, chitosan [48] and egg shell membrane [50] have used as templates to prepare high surface porous alumina matrices that can contain remaining moieties from the templating biopolymer which assists to CA immobilization. In overall, those that studied reusability in biopolymer/composite materials reported considerable reduction of activity within a small number of reusability cycles as in the case of inorganic matrices. To conclude, absorption is an easy immobilization procedure that yields recyclable heterogeneous biocatalysts which main disadvantages are eventual desorption and nonspecific adsorption (prior enzyme purification). However, enzyme modification and appropriate carrier selection can overcome these issues as some examples have shown.

2.2. *Covalent attachment to surface modified materials*

Carrier surface functionalization allows enzyme immobilization by covalent bonding. Covalent attachment is characterized by improved immobilized enzyme stability and reusability [30]. While improvements in reusability are due to the enzyme-material connection strength, protein stabilization is related to an enzyme conformational stiffening upon (multy)-covalent linkage to support's surface [51]. Some important routs of covalent enzyme immobilization are summarized in Fig. 3. Several kinds of configurations have been investigated in the literature to attach covalently CA on a carrier surface: porous solids, nanoparticles and nanofibers. Increasing the specific surface is an essential requirement when thinking of further scaling up and application of the material. In the following, an overview of each configuration is presented.

2.2.1. *Porous solids*

The use of high porosity materials allows having large surface to mass ratios. Since the surface is well covered by functional groups, large enzyme loadings are possible. Both inorganic and organic materials have been tested as support for CA. Within the first group, examples are SiO_2 based materials such as controlled pore glasses [23], SBA-15 mesoporous silica [52], glass coated iron fillings [53] and a hero-functional

Table 1
Properties of immobilized carbonic anhydrase.

Immobilization method	CA type	Immobilization material	Activity	Thermal stability	Storage	Reusability	Loading	Ref
Adsorption	Bovine	Mesoporous molecular sieves, 1–D material 3 nm pore	82(M)	–	78/68 (6 d, 40 °C, M)	–	52	[35]
	Bovine	Mesoporous molecular sieves (SBA-15), 2–D material 5−15 nm pore	78(M)	–	96/68 (6 d, 40 °C, M)	–	61	[35]
	Bovine	Mesoporous molecular sieves, 3–D material 6.5 nm pore	36(M)	–	88/68 (6 d, 40 °C, M)	–	47	[35]
	Partially purified	Mesoporous aluminosilicates	~17.8(CO2) ~48.8 (Ca)	~35/19 (4 h, 55 °C, p)	>50/20 (25 d, 25 °C, p)	19 % (10 c, Ca)	–	[39]
	Bovine	SBA – 15 (silica) mesoporous	~47.9(CO2)^ ~92.9 (Ca)	–	–	50 % (10 c, CO2)	96	[40]
	Human	Supported silver nanoparticles	~98.8(p)^ ~96.6(Ca)	–	89/77 (30 d, 25 °C, Ca)	84 % (30 c, Ca)	307	[41]
	Human	Supported gold nanoparticles	~96.9(p)^ ~97.0(Ca)	–	98/69 (20 d, 25 °C, p)	96 % (20 c, p)	289.13	[42]
	Peptide tagged	Silica particles	~100(p)	~58/28 (30 min, 55 °C, p)	90/70 (10 d, 4 °C, p)	95 % (5 c, p)	2.5	[37]
	Peptide tagged	Titania particles	~100(p)	~84/28 (30 min, 55 °C, p)	95/70 (10 d, 4 °C, p)	95 % (5 c, p)	3.74	[37]
	Partially unfolded bovine	Octyl – substituted Sepharose 4B	~700(p)	~69/16 (1.33 h, 65 °C, p), refered to initial	–	–	–	[44]
	Bacterial, partially purified	Chitosan glutaraldehyde cross – linked beads	~34.9(CO2) ~21.4(p)^ ~78.7(Ca)	~9.73/? (8 h, 55 °C, p)	Half life (25 °C), free 408 h Immobilized 456 h	~54.5 % (9 c, Ca)	–	[45]
	Whole cell, CA enriched microorganism	Chitosan beads (NH_4OH)	~154.4(p) compared to free culture ~70.7(p) compared to CA purified	–	–	–	–	[46]
	Partially purified bacterial	Chitosan – clay beads	~92.4(p)	–	–	–	–	[46]
	Bacterial	Chitosan beads (KOH)	89(CO2)	68/59 (3 h, 55 °C, CO2), referred to initial	83/41 (30 d, 4 °C, CO2)	~12 % (7 c, Ca)	4.4	[47]
	Whole cell, CA enriched microorganism	Chitosan beads (NH_4OH)	75(CO2) compared to free culture	–	–	–	7.4	[47]
	Bacterial	$CaCl_2$ cross – linked) sodium alginate	38(CO2)	–	–	–	1.9	[47]
	Partially purified bacterial	Chitosan stabilized iron nanoparticles	~12.18(CO2) ~83.97 (p)^ ~61.71 (Ca)	~78/18 (?, 55 °C, p)	65/ 43 (20 d, room T,p)	50 % (5 c, p)	23.2	[38]
	Partially purified	Chitosan based carbon – alumina beads	~18.26(p)^ ~85.14(Ca)	~92/38 (4 h, 55 °C, p)	~40/37 (25 d, 4 °C, p)	50 % (4 c, p)	~30.6	[48]
	Bacterial crude extract	Mesoporous alumina – egg shell membrane matrix	~31.00(p)^ ~17.18 (CO2) ~75.16(Ca)	~35/35 (4 h, 55 °C, p)	Half-life (25 °C), free 480 h, immobilized 600 h	~34 % (10 c, Ca)	–	[50]
Covalent bonding to surface modified materials	Bovine	Activated carbon (70 %v <2 nm and 20 %v 2−20 nm pores)	0.229(M)	~62/34 (90 d, 50 °C, M), referred to initial	–	–	18.3	[23]
	Bovine	Controlled pore glass (38 nm)	0.351(p) 0.209(M)	~65/34 (90 d, 50 °C, M) 33/37 (90 d, 50 °C, p), referred to initial	–	–	32.6	[23]
	Bovine	Controlled pore glass (100 nm)	0.383(p) 0.159(M)	~91/34 (90 d, 50 °C, M) ~12/37 (90 d, 50 °C, p), referred to initial	–	–	10.7	[23]
	Bovine	Aluminum oxide	–	~78/24 (at 70 °C, no incubation, p)	–	>80 % (40 c, p)	–	[55]
	Thermostable	Heterofunctionalized support (containing $CaCO_3$_H_3BO_3 − SiO_2) and a Zn complex	~1.89 support ~2.09 immobilized CA, ~2.52 immobilized CA + Zn complex. Improvement	~73/60 (1 h, 90 °C, p)	Minor lost (1 week, 25 °C, MEA)	>90 % (15 c, CO2 gravimetric)	107.5	[54]

(*continued on next page*)

Table 1 (*continued*)

Immobilization method	CA type	Immobilization material	Activity	Thermal stability	Storage	Reusability	Loading	Ref
			factors in CO_2 absorption flux with respect to neat solvent					
	Human	SBA − 15 (silica) mesoporous	~97.4(p)ˆ ~98.9(Ca)	~86/70 (at 50 °C, no incubation, p)	92/65 (30 d, 30 °C, p)	~87.5 % (40 c, p) ~78.8 % (40 c, Ca)	291	[52]
	Bovine	Iron fillings	>98(CO2)	~39/18 (25 min, 65 °C, CO2), referred to initial	~75/57 (50 d, 35 °C, CO2)	~44 % (50 c, CO2)	–	[53]
	Bovine	Glass coated iron fillings	>98(CO2)	~33/18 (25 min, 65 °C, CO2), referred to initial	~69/57 (50 d, 35 °C, CO2)	~33 % (50 c, CO2)	–	[53]
	Bovine	Co − polymer methacrylic acid − methacrylic m − fluoroanilide nitrate beads	>98(CO2)	~29/18 (25 min, 65 °C, CO2), referred to initial	~67/57 (50 d, 35 °C, CO2)	~30 % (50 c, CO2)	–	[53]
	Bovine	Water plasma treated PVDF membrane, amine functionalized	60(p)+ 42.2(p)ˆ 76(Ca)	–	70.4/12.0 (30 d, 25 °C, p)	85.8 % (10 c, p)	–	[56]
	Bovine	Water plasma treated PVDF membrane, epoxy fuctionlized	33(p)+ 24.0(p)ˆ 65(Ca)	–	~63.8/12.0 (30 d, 25 °C, p)	71.5 % (10 c, p)	–	[56]
	Bovine	Polyethylenimine − dopamine coated PVDF membrane	53.40(p)+ ~27.1(p)ˆ 63.3 (Ca)	–	63.46/ 54 (30 d, 25 °C, p)	77.52 % (10 c, p)	–	[57]
	Bovine	Polyethylenimine − dopamine coated PP membrane	75.86(p)+ ~64.1(p)ˆ 85.4(Ca)	–	75.21/ 54 (30 d, 25 °C, p)	81.35 % (10 c, p)	–	[57]
	Human	Electropolymerized porous carbon	–	40/8 (1 h, 70 °C, p)	50/- (42 d, 70°, p) in 1 M MDEA	–	–	[58]
	Bovine	Nonporous silica nanoparticles	47(M)ˆ	~100/24(at 50 °C, no incubation, M)	38/3 (30 d, 50 °C, M)	–	54.9	[60]
	Bovine	TiO_2 nanoparticles	87.6 (p)+ ~73.4(p)ˆ ~95.45 (Ca)	–	~72/41 (20 d, 25 °C, p)	85 % (20 c, p)	163	[62]
	Bovine	Magnetic polymeric microspheres	~22.25(p)ˆ	~100/0 (1 h, 70 °C, p) ~100/70 (20 min, 70 °C, p), referred to initial	90.9/71.8 (30 d, 4 °C, p)	47.6 % (6 c, p)	–	[64]
	Recombinant bacterial	Iron magnetic nanoparticles	Shorter precipitation onset than free (Ca)	50/0 (30 min, 70 °C, CO2) ~79/49(30 min, 60 °C, CO2)	<100 (minor lost) /100 (28 d, 4 °C, CO2)	50 % (22 c, CO2)	~570	[65]
	Thermostable	Iron magnetic nanoparticles	47(M)ˆ in 0.5 M Na_2CO_3-$NaHCO_3$	~95/3 (70 h, 70 °C, CO2), referred to initial	~94/30 (30 d, 25 °C, CO2)	–	40	[66]
	Human	Silica coated iron oxide magnetic nanoparticles	~3.08(p)ˆ	35/24 (1.5 h, 50 °C, p), referred to initial	85/0.11 (40 d, 25 °C, p)	61 % (13 c, p)	–	[67]
	Thermostable recombinant	Iron oxide magnetic nanoparticles	~2.08(CO2)	100/30 (70 h, 70 °C, CO2)	100/25 (30 d, 25 °C, CO2)	–	~48	[68]
	Bovine	Iron oxide magnetic nanoparticles	~2.08(CO2)	~20/0 (70 h, 70 °C, CO2)	50/0 (30 d, 25 °C, CO2)	–	~48	[68]
	Purified recombinant thermostable	Electrospun nanofibers (PE − PAN)	~17.60(CO2)	~51/42 (15 min, 80 °C, CO2)	–	8% (5 c, CO2)	–	[69]
Cross-linked enzyme aggregates	Bovine	Supported CLEA in magnetic nanoparticles	36(CO2) ~1.31 (M)	–	–	95 % (5 c, M)	~1680	[73]
	Bovine	Supported CLEA in electrospun nanofibers	~8.88(p) ~2.73 (p)ˆ	–	65.3/0 (868 d, room T, p)	–	916	[71]
	Bovine	Unsupported CLEA	~19.19 (p)ˆ	–	–	–	–	[71]
	Bovine	CA covalently immobilized in nanofibers (not surface modification)	~9.07(p) ~8.22(p)ˆ	–	7.2/8.7 (7 d, room T, p)	–	11.4	[71]

(*continued on next page*)

Table 1 (*continued*)

Immobilization method	CA type	Immobilization material	Activity	Thermal stability	Storage	Reusability	Loading	Ref
	Bovine	SBA − 15 (silica) mesoporous	~95.6(CO2)ˆ ~98.6(Ca)	~82/71 (at 50 °C no incubation, CO2)ˆ	95/45 (30 d, 25 °C, CO2)	97 % (10 c, CO2)	193	[40]
Enzyme co − polymer	Bovine	Polyester − polyurethane prepolymer 80	59.82(p)+	40.18/14.25 (1 h, 60 °C, p)	86.79/22.34 (14 d, 4 °C, p) 55.56/6.2 (14 d, 25 °C, p)	58.1 % (5 c, p)	–	[77]
	Bovine	Polyurethane prepolymer HYPOL2060	Km free 12.2 mM, Km immobilized 9.6 mM (p)	–	100/0 (45 d, room temperature for immobilized, 4 °C for free, p)	100 % (7 c, p)	–	[78]
	Bovine	Silk fibroin − based hydrogels	>60(p)	–	–	–	–	[79]
Entrapment	Bovine	Alginate beads (millimetric size)	~0.007(CO2)	~ 90/55 (at 40 °C no incubation, CO2)	~74/31 (21 d, 4 °C, CO2) ~54/24 (21 d, 25 °C, CO2)	67 % (6 c, CO2)	1160	[81]
	Bovine	Chitosan coated alginate beads	~30.8(p)+	~35.7/7.1 (3 h, 70 °C, p), referred to initial	–	? % (15 c, Ca)	–	[49, 83]
	Purified bacterial	Chitosan − alginate polyelectrolyte complex beads	94.5(CO2) ~94.8(Ca) ~91.5(p)ˆ	43/0 (2 h, 70 °C, CO2)	100/0 (28 d, 4 °C, CO2)	53% (8 c, CO2)	–	[109]
	Bovine	Glutaraldehyde cross − linked alginate beads	56.3(CO2)+	40/7 (1 h, 60 °C, CO2)	87/67.8 (20 d, 30 °C, CO2)	61 % (6 c, absorption)	–	[82]
	Bovine	Poly(acrylic acid − acrylamide) − hydrotalcite nanocomposites	90.9(CO2)	65/0 (1 h, 50 °C, CO2), referred to initial	–	–	~2.7	[86, 85]
	Bovine	Polyacrylamide gel microparticles	~71.1(p)ˆ	>25/0 (30 min, 110 °C, p)	–	–	–	[87]
	Bovine	Polyacryldextran microspheres	~69.5(p)ˆ	50/0 (30 min, 65 °C, p) 5−10/0 (30 min, 100 °C, p)	–	–	–	[88]
	Bovine	Silica monolith	1(p)	–	–	–	–	[89]
	Bovine	Silica nanoparticles	58(p) ~48.9(p)ˆ ~93.2 (Ca)	~ 95/0 (at 50 °C no incubation, p) Using 40 °C as optimum	Very good/? (1 w, 20 °C, p)	87 % (5 c, p)	~298 (23 $\%_w$)	[90]
MOF	No specified	ZIF − L, co − precipitation	150(M) 1 M MDEA	~75/54 (20 d, 40 °C, M) in 1 M MDEA, referred to initial	–	89.3 % (6 c, M)	67	[94]
	Bovine	ZIF − 8, co − precipitation	118(p)ˆ ~116.3(Ca)	86/55 (1 h, 55 °C, p)	89/47 (37 d, room temperature, p)	84 % (12 c, p) ~55 % (10 c, Ca)	100	[95]
	Bovine	ZIF − 8, adsorption	36(p) ~25.8(p)ˆ	~70/57 (30 min, 70 °C, p)	75/50 (30 d, room temperature, p)	–	54	[34]
	Bovine	MIL − 160, adsorption	72(p) ~78.6(p)ˆ	~93/57 (30 min, 70 °C, p)	80/50 (30 d, room temperature, p)	–	35	[34]
	Bovine	ZIF − 8, adsorption	75(p)+ ~94.2(p)ˆ	~33/10 (1 h, 60 °C, p), referred to initial	–	85 % (9 c, p)	–	[97]
	Bovine	ZIF − 8, co − precipitation	–	~79/25 (30 min, 65 °C, p), referred to initial	–	0% (11 c, p)	–	[96]
	Bovine	ZIF − 8, co − precipitation embedded in a poly(vinyl alcohol) − chitosan membrane	–	~98/25 (30 min, 65 °C, p), referred to initial	–	50 % (11 c, p)	–	[96]
		Ni based MOF, adsorption	98.99(p)+ ~87.8(p)ˆ			65 % (8 c, p)	–	[98]

(*continued on next page*)

Table 1 (*continued*)

Immobilization method	CA type	Immobilization material	Activity	Thermal stability	Storage	Reusability	Loading	Ref
	Recombinant human with a His tag, crude lysate			~93/54 (4 h, 50 °C, p) Using 40 °C as optimun	41.8/6.4 (10 d, 25 °C, p)			
Nanoflowers	Bovine	$Cu_3(PO_4)_2.3H_2O$	~261(CO2)	–	–	–	–	[101]
	Bovine	$Ca_8H_2(PO_4)_6$	149(p) ~47.26(p)^	~42/0 (1 h, 80 °C, p)	–	~100 % (5 c, Ca)	–	[102]
	Bovine	$Mn_3(PO_4)_2$	~30.0(p) ~80.4(p)^	~32/0 (1 h, 80 °C, p)	–	~38 % (5 c, Ca)	–	[102]
	Bovine	$Cu_3(PO_4)_2$	286(p) ~154.9 (p)^	~17/0 (1 h, 80 °C, p)	–	~100 % (5 c, Ca)	–	[102]
	No specified	$Cu_3(PO_4)_2$	~7(p)+	–	–	–	–	[107]
	No specified	$Zn_3(PO_4)_2$	35(p)+	–	–	–	–	[107]
	No specified	$(Zn-Cu)_3(PO_4)_2$	70(p)+	~33/7 (25 min, 65 °C, p), referred to initial	56/22 (18 d, 25 °C,p)	13 % (8c, p)	–	[107]
	No specified	$(Zn-Cu)_3(PO_4)_2$ embedded in a poly(vinyl alcohol) − chitosan membrane	~41(p)+	~43/7 (25 min, 65 °C, p), referred to initial	88/22 (18 d, 25 °C,p)	75 % (8c, p)	–	[107]

Column information legend:

- Activity column: activity with respect to free enzyme in % (measuring technique). When no indicated, activity is expressed as efficiency [26] or +, activity is expressed as activity recovery [26] while ^, activity is expressed as kcat/Km or Vmax/Km immobilized to free enzyme ratio.
- Thermal stability column: relative (to the maximum) immobilized CA activity/relative free enzyme activity in % (incubation time, temperature, measuring technique).
- Storage column: relative (to the initial) immobilized CA activity/relative free enzyme activity in % (storage time, storage temperature, measuring technique).
- Reusability column: relative (to the first cycle) immobilized CA activity (cycle at which the activity is reported, measuring technique).
- Loading: CA concentration in mg/g immobilized CA.

Activity measuring method legend:

- M, manometric.
- p, p − NPA hydrolysis.
- CO2, CO_2 hydration.
- Ca, $CaCO_3$ precipitation.

Values preceded by ~ are computed/estimated based on the data provided. Data from graphs was extracted using the free online software WebPlotDigitizer [110].

support consisting of $CaCO_3/H_3BO_3/SiO_2$ [54]; iron fillings [53]; aluminium oxide beads [55] and activated carbon [23]. For most of them, surface functionalization is conducted by reacting superficial −OH groups with an amino/epoxy/carboxylic functionalized silane. Once the surface contains the desired functional groups immobilization is performed according to what is shown in Fig. 3. As discussed by Vinoba et al. [52], different functional groups can provide different results. They studied amine functionalized SBA-15 (silica) mesoporous supports with three different amine moieties. Although they shown slight differences in efficiency, storage and thermal stability and reusability, their loading capacity was different. Loading was not directly correlated with differences in specific surface, pore volume or pore diameter but to the chemical structure of amine groups at the carrier surface. With regards to polymeric materials, some authors have focused on hydrophobic polymeric membranes such as PVDF or PP which are commonly used in gas-liquid membrane contactors for absorption. Due to their inertness, more complex immobilization routes are required in order to incorporate the moieties on their surface. For example, Sun et al. [56] prepared PVDF flat membranes modified by water plasma. This technique introduced hydroxyl groups on the surface. Then, the membrane was amine or epoxy functionalized by silanes. Again, different surface groups provide different results. Later on, the same group [57] immobilized CA by covalent bounding to the surface of a glutaraldehyde modified PVDF and PE membranes. They first deposited polyethyleneimine and polydopamine on the membrane surface. This coating contains the required $–NH_2$ groups. In both studies, the effect of superficial functional group density was analyzed. The larger the density, the more enzyme can bond to the surface increasing the loading. A plateau is reached at some point because of steric hindrance between enzymes. Finally, Merle et al. [58] coated a highly porous carbon based support (carbon foam) with a electropolymerized polymer film (poly (aminopropyl)pyrrole) to which CA was later covalently immobilized. CA was either directly join to the coating or connected through a PEO spacer. The later approach was more successful in terms of loading and activity as it reduced steric hindrance between enzymes and provided better substrate accessibility to the enzyme. As covalent binging is not site specific, enzyme orientation is random when it joints to the support. Thus, the active center of some enzyme might be facing the surface limiting reactants accessibility [59]. The use of a spacer solves this issue. As expected, carriers discussed so far present better reusability than in the case of immobilization via absorption. Here, activity reduction during reutilization is not completely due to leaching but to enzyme alteration after being exposed to reactants/products [53].

2.2.2. *Nanoparticles and nanofibers*

An alternative approach to porous solids is the use of nanoparticles. Immobilization on nanoparticles presents the advantages of higher surface to mass ratios than bigger particles (high loading) and reduced intraparticle diffusional resistance [60,61]. However, small size makes more challenging their recovery. This problem is overcome when using magnetic nanoparticles which are easily separated by a magnetic field. Among the examples that can be discussed of non-magnetic nanoparticles are nonporous silica [60] and TiO_2 [62] nanoparticles. Different nonporous silica nanoparticle sizes were studied by Zhang and Ye [60]. Loading, activity and thermal stability were higher for the smallest particles. While loading is due to larger specify surface, higher activities in smaller nanoparticles could be related to a reduction in enzyme - particle surface interaction. These interactions can have an effect in enzyme's secondary structure [63]. They also compared their results to their previous work in controlled pore glass materials [23] included in the previous section. With nonporous nanoparticles, larger activities (double) and loadings were obtained. Magnetic nanoparticles based either on epoxy [64] or amine [65–68] functionalized iron oxide have been also studied. Although showing an activity reduction upon

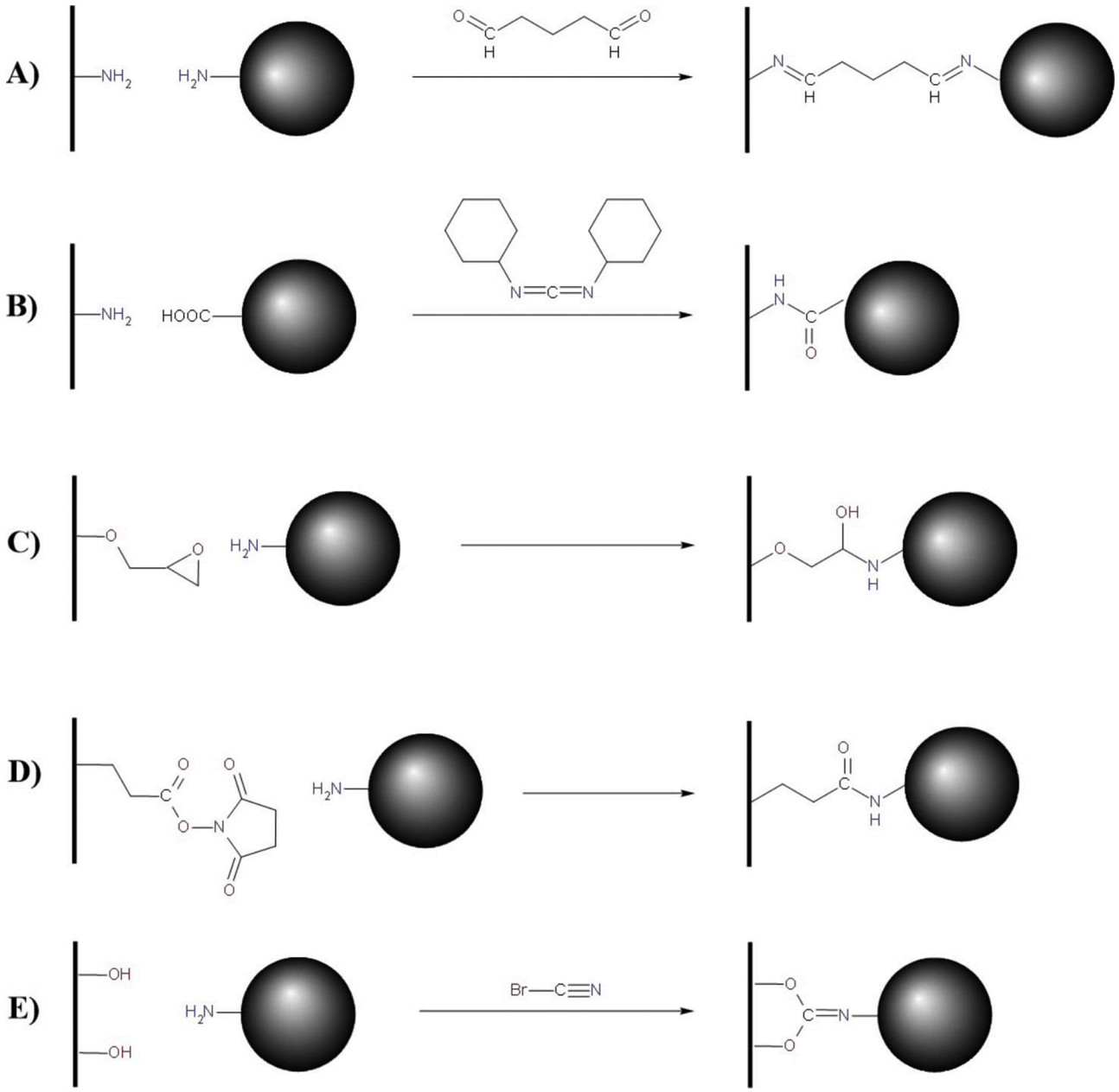

Fig. 3. Overview of different enzyme immobilization rutes to functionalized carriers. (A) amine - amine reaction through glutaraldehyde, (B) carbodiimide activation to allow amine - carboxylic reaction, (C) direct amine – epoxy reaction, (D) direct 4-N-hydroxysuccinimide – amine reaction and (E) cyanogen bromide activation to allow hydroxyl – amine reaction.

immobilization, enzyme structural stiffening provides a significant improvement in thermal stability compared to free enzyme. Based in a comparison of characteristic time of reaction and diffusion in nonporous nanoparticles i.e. transport from liquid bulk to nanoparticle surface, Pierce et al. [66] showed that activity reduction was not caused by mass transfer limitations but slower intrinsic kinetics of the immobilized CA. Therefore, lower efficiency was due to enzyme deformation during covalent attachment. Another factor to consider as reason of activity reduction compared to free enzyme is nanoparticle aggregation [68]. Concerning nanofibers, electrospun nanofibers present the main advantages of nanoparticles but at the same time, there are separated more easily. So far, they have received less attention than nanoparticles for CA immobilization. As an example, S. Effendi et al. [69] immobilized covalently CA into a composite membrane made of PAN and PET nanofibers produced by electrospinning. They immobilized CA in a purified form or directly from and crude extract. While purified presented higher activity its thermal stability was lower than crude CA which is interesting considering CA purification cost and requirements in thermal stability for post-combustion CO_2 capture. However, this immobilized biocatalyst did not present a good reusability.

In conclusion, despite that immobilized enzyme catalytic properties will depend on the CA type, carrier and immobilization protocol, surface modified materials for CA immobilization generally present the advantage of attaining high loading, reusability and improved thermal stability. Complexity associated to surface modification which usually requires longer immobilization procedures and the possibility of enzyme structure alteration via covalent attachment are its main threats. Each step of the immobilization needs to be optimized in order to attain the best properties and chemicals often used such us glutaraldehyde can cause harm to human health [70].

2.3. Cross-linked enzyme aggregates

The idea behind cross-linked enzyme aggregates or CLEAs is to remove the enzyme support and to have a completely active material made of enzymes that are supporting themselves. Large activities per g of heterogeneous biocatalyst are thus expected. In order to prepare them, the enzyme is precipitated using a precipitation agent and incubated with a cross-linking agent such as glutaraldehyde [71]. Then, the conglomerate of enzyme forming the precipitates is cross-linked forming a 3D network of enzymes covalently interconnected. Precipitation can be performed directly from a crude extract reducing enzyme purification cost [26]. Because of CLEA softness and easy breakage, a combination of surface modified covalent attachment and CLEAs has been used to prepare supported CLEAs [72]. This later approach has received more attention in CA immobilization. For example, Peirce et al. [73,74] prepared CA CLEAs and magnetic nanoparticle supported CLEAs. They optimized the immobilization procedure (temperature, time, glutaraldehyde concentration, precipitation agent, enzyme/support ratio and stirring conditions) in order to attain the best yield and specific activity. In a study by Jun et al. [71], the use of electrospun polymer nanofibers as CLEA support was analyzed. The storage stability of elecstrospun nanofiber supported CLEA was remarkably superior to the surface covalently linked CA (enzyme monolayer) and free enzyme. Stabilization was further investigated by Zn leaching tests with EDTA and Molecular Dynamic Simulations. Observed differences in activity between free, unsupported CLEA, supported CLEA and surface covalently linked CA were due to mass transfer limitations and enzyme conformational alteration due to multipoint enzyme cross-linking. Interestingly, Vinoba et al. [40] prepared spherical SBA-15 (mesoporous silica) and compared its performance as carrier for CA adsorption, surface covalent attachment and supported CLEAs. Supported CLEAs provided the best results in terms of loading, efficiency and reutilization. To sum up, CLEAs have the highest loadings among all immobilization methods. Although there are limited examples for CA immobilization, CLEAs are generally characterized by a high enzyme stabilization (temperature, pH, realization, storage, organic solvents, etc.) [75,76] which makes them attractive for harsh conditions in CO_2 capture. However, they share the main disadvantages of covalent bonding methods and they can present diffusional limitations in the cross-linked matrix [30]. As CO_2 is a small substrate, this resistance may be less important.

2.4. Enzyme co-polymerization

CA can also be incorporated as part of the polymerization formulation (co-polymerization). This requires the monomer to contain functional groups that can react with the enzyme. Here, CA is not just covalently bound at the surface but also in the interior of the material. Therefore, this immobilization method lies between entrapment and covalent bonding. As example of synthetic polymers, some authors have carried out co-polymerization of different polyurethane prepolymers in the presence of CA [77,78]. Polyurethane contains isocyanate groups that can directly react with $–NH_2$ and $–OH$ groups at enzyme's surface. As these prepolymers are already commercially available, the immobilization process is straightforward. However, in order to arrive to the best activity it should be optimized [77]. These porous materials showed improved reusability, thermal and storage stability. Because of the strong carrier-enzyme connection enzyme leaching from the porous soft and hydrophilic polymer is avoided. Concerning biopolymers, Han et al. [79] immobilized CA into silk fibroin-based biohydrogels prepared by a Ru(II) mediated photochemical reaction. Tyrosine residues from CA were cross-linked to those present in the silk forming a cross-linked hydrogel with covalently bounded CA. A very high immobilization yield was observed which is not the case of conventional physical entrapment. An efficiency lower than 100% could have been caused by mass transfer limitation due to diffusion inside of the hydrogels, different microenvironment and/or enzyme conformational change during immobilization. None of the cited studied reports loading, however because of the abundance of functional groups to which CA can be covalently linked it is expected to have higher loadings than in entrapment.

2.5. Entrapment

Enzyme immobilization through entrapment is based on its physical confinement within the material. Biopolymers and hydrogels have been extensively studied as carriers for entrapment [26]. Biopolymers are non-toxic, cheap, available, hydrophilic and present good enzyme compatibility [80]. In this case, enzyme is generally immobilized through imprisonment between the biopolymeric chains. For some biopolymers commonly used such as chitosan or alginate, the immobilization methodology is generally straightforward and simple (see the references included in this section). Because of its high porosity (reduction of intraparticle mass transfer limitations) alginate beads have been a popular choice as entrapment biopolymer [81,82]. However, alginate beads shown a large percentage of activity reduction during recycling, probably due to enzyme leaching from the soft and porous matrix. To prevent this, Simsek-Ege et al. [49,83,84] prepared chitosan coated alginate beads with entrapped CA. They optimized the immobilization process in order to reduce losses during beads preparation (low yield) and at longer term (leaching). With regards to other hydrogels, Zhang et al. [85,86] developed poly(acrylic acid-co-acrylamide)/hydrotalcite (PAA-AAm/HT) nanocomposite hydrogels in which CA was either entrapped or covalently bounded via hydrogel activation. Enzyme loading and thermal stabilization was lower compared to covalent attachment but the specific activity was significantly higher indicating lower enzyme deactivation. Aqueous microenvironments within the porous hydrogel were a compatible environment for CA leading to high efficiency. Another example although no linked to CO_2 capture is the study performed by Edman et al. [87] that prepared polyacrylamide gel highly cross-linked microparticles via emulsion polymerization. CA was incorporated in the monomer solution to ensure embedding. High degree of crosslinking can strongly reduce leaching while affecting negatively to mass transfer within the material. The use of microparticles reduces this issue. They reported a very large thermal stabilization. When imprisoned between polymeric chains enzyme structural changes are sterically hindered causing an improvement in stability. However, it is highlighted that a large portion of enzyme was wasted during their preparation (low yield). Later, the same authors [88] studied as CA carrier biodegradable microspheres of polyacryldextran. The optimized polymerization composition to increase yield although long term leaching was still a problem. Silica sol-gel materials have the predominant position within inorganic materials applied for CA entrapment [89–91]. Silica gels preparation is a mild, simple, one-step process in which gel properties such as porosity and superficial functional groups can be tuned. In contrast, to previously discussed examples, Forsyth et al. [90] reported 100% yield, low enzyme leaching and good reusability. Silica gel 3D network formation around the enzymes ensures strong entrapment [91]. As shown by CD measurements, CA conformation is identical to in free solution indicating that the interior of the gel is a good microenvironment [89]. Because of the restricted CA mobility and separation of enzyme molecules, unfolding and subsequent irreversible aggregation and precipitation (main steps in enzyme denaturation) are avoided leading to improved thermal stability compared to free enzyme [89,90]. It can be concluded that in entrapment, the immobilized enzyme continues its catalytic activity inside of aqueous microenvironments. Thus, this immobilization strategy ensures lower risk of enzyme deactivation compared to other methods such as covalent bonding. Due to steric hindrance, conformation changes are limited improving immobilized enzyme thermal stability. However, the main drawbacks of this immobilization method are enzyme leaching from the soft matrix, diffusional limitations of reactants/products and partition coefficient of these

compounds between the matrix and the aqueous solution.

2.6. Metal organic frameworks

Metal Organic Frameworks (MOFs) are novel high-surface porous crystalline materials formed by the coordination of metal ions with organic ligands. The choice of metals and ligands allows easily tuning of properties such as pore size and surface functional groups [92]. The application of MOFs into biocatalysts is still a very novel approach. Yet, MOFs have provided unprecedented results because in some cases it is possible to obtained higher activities for immobilized than free enzyme and extraordinary stability enhancements [93,94]. The mild fabrication conditions of some MOFs such us Zeolitic Imidazolate Framework (ZIFs) permit to include the enzyme in their formulation. Four immobilization pathways are possible: surface adsorption, surface covalent bonding, pore encapsulation (mesoporous MOF's cavity) and co-precipitation or in situ encapsulation (entrapment within crystalline structural defects) [93], see Fig. 4. The effects in CA conformation upon immobilization and their consequences in activity and stability will depend on the pathway followed. Up to now, CA has been immobilized either by co-precipitation [94–96] or adsorption [34,97,98]. Zhang et al. [94] and Asadi et al. [95] prepared ZIF with immobilized CA by co-precipitation. They both reported higher specific activities for immobilized than free enzyme although enzyme structure was not altered upon immobilization in any of them. Observed activity enhancements could be due to enzyme activation by CA – carrier interactions or by substrate/product – carrier interactions such as positive partition coefficients or reduced enzyme inhibition [99]. ZIF contains imidazole groups that can catalyze CO_2 hydration which can explain why these materials surpass free enzyme. Nevertheless, as shown by Zhang et al. [94], this improvement is rather small compared to synergic effect of combining both CA and ZIF-8 (50% larger than free enzyme). They also reported improvements in thermal stability and good reusability. With regards to adsorption, Liu et al. [34] compared two different MOFs as support materials: one hydrophobic, ZIF-8 and one hydrophilic, aluminum based MIL-160. The best results were obtained for the hydrophilic MOF. Because CA contains more hydrophilic moieties in its surface, its structure was more disrupted when immobilized on the hydrophobic MOF. Another example is the study by Jiao et al. [98]. They investigated Ni-Based MOF nanorods in which CA was immobilized. To improve CA – Ni interaction, the modified Human CA with a His-tag allowing direct adsorption from the cell lysate. However, at higher temperatures enzyme leaching reduced the immobilized CA apparent thermal stability with regards to free CA. To conclude, as it has been discussed, synergy between CA and MOF can lead to efficiencies higher than 100% making these carries very attractive because less enzyme will be required. MOFs tunable structure and novelty ensures room for further improvement in CA-MOF properties. However, MOFs small size and low mechanical strength is still a challenge [96]. Aiming to address this issue, Ren et al. [96] embedded the immobilized enzyme into a poly (vinyl) alcohol-chitosan membrane improving its stability, reusability and mechanical properties.

2.7. Nanoflowers

Self-assembly hybrid nanoflower materials have been discovered recently (2012) as a new type of immobilization approach [101]. Their typical flower like structure is formed by enzyme-metal coordination during metallic phosphate crystallization, see Fig. 5. These materials are remarkable by their easy preparation (one step procedure) and their impressive results in terms of improved enzyme activity/stability compared to free enzyme in some cases [101,102]. In the paper describing this discovery, among other enzymes, CA was immobilized in $Cu_3(PO_4)_2.3H_2O$ nanoflowers. Despite of the low yield (10%), the efficiency for CO_2 hydration was around 260% [101]. The authors explained that this enhancement is due to nanoflower high specific surface and nanoscale enzyme confinement. Apart from Cu^{2+}, other metallic cations that have been used including Mn^{2+}, Ca^{2+} and Zn^{2+} [103]. Duan et al. [102] compared Ca^{+2}, Cu^{+2} and Mn^{+2} based hybrid nanoflower like materials. Both Ca^{2+} and Cu^{2+} overcome free enzyme while for Mn^{2+} efficiency was lower than 100%. The authors indicated that these metals activate CA perhaps through metal exchange with the Zn^{2+} cation at the active center. Although low yields were reported, the immobilized CA presented good reusability and thermal stability. CA interaction with metallic cations is a complex subject [104]. Cu^{+2}, for example, can join to the active site but also to other regions of CA [105]. It has been observed that replacing the native Zn^{2+} cation by other metals such as Co^{2+}, Cu^{2+}, Cd^{2+} or Ni^{2+} leads to minimal conformational changes although the activity is decreased compared to Zn^{2+} [106]. None of the studies focused on CA immobilization in nanoflowers have studied the effect of immobilization in enzyme conformation. However, since the enzyme is immobilized through entrapment, we can expect that sterically restricted enzyme conformational changes due to nanoconfinement might contribute to immobilized CA stability. Wen et al. [107] prepared bimetallic hydrid nanoflowers. In this publication, bimetallic refers to Cu and Zn instead of a simple metallic cation, although hybrids containing only Cu and Zn were used as comparison. Including both metals produced a synergic effect in terms of activity recovery. When studying its reusability, this immobilized biocatalyst suffers an important loss of activity during the first 8 cycles. Similarly to MOFs, hybrid nanoflowers are small and brittle. Therefore, it is possible to damage the material during reutilization. Again, entrapping the nanoflowers in a poly (vinyl) alcohol-chitosan membrane improved reusability but also thermal and storage stability [107]. Although it is a very new field, immobilization in hybrid nanoflowers is a promising approach. However, for their industrial implementation their low mechanical stability must be considered.

3. Technologies to capture CO_2 using immobilized carbonic anhydrase

While the first part of this article has been focused on reviewing CA immobilization, the second one focuses on the different technologies that are under development or already in the industry that use

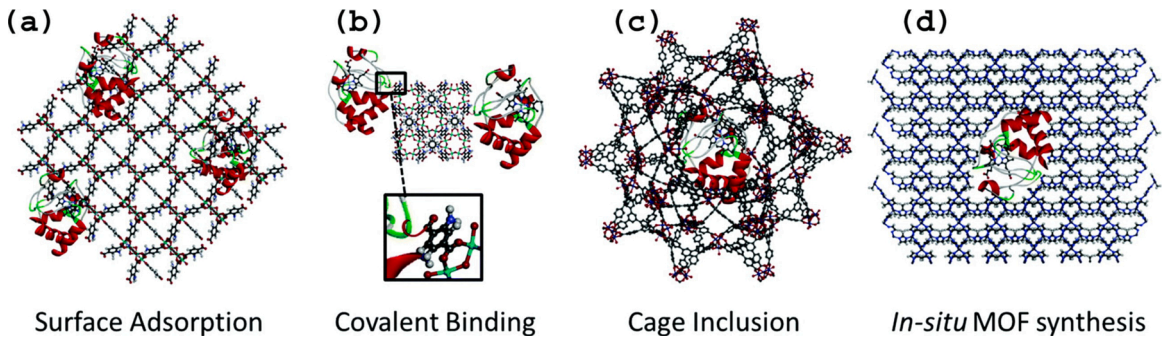

Fig. 4. Enzyme immobilization strategies in MOFs. Reprinted from [100] with the permission of the Royal Society of Chemistry. Copyright (2017).

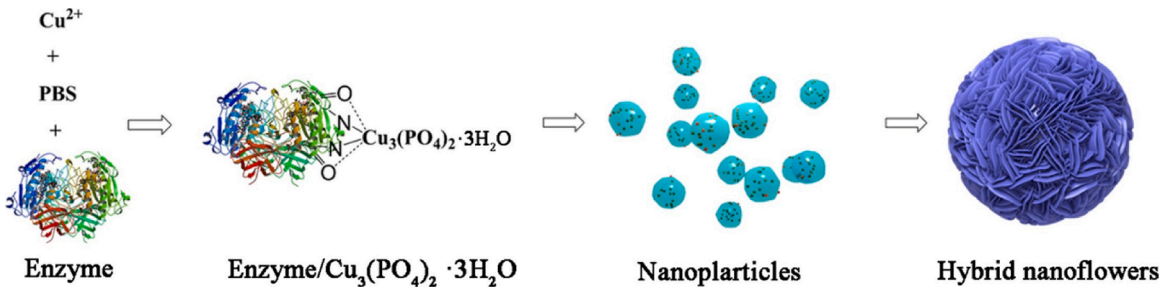

Fig. 5. Nanoflowers formation process. The enzyme coordinated to metallic phosphate becomes a nucleus from which crystalline nanoflowers grow. Reprinted from [108] with the permission of Elsevier. Copyright (2016).

immobilized CA to enhance CO_2 separation. So far, two main CO_2 capture processes are the spotlight using CA: gas absorption and selective membrane separation. Therefore, this section will cover these technologies. This section is structured as follows: first, a brief introduction to the mass transfer theory to consider in each capture process indicating the reference to which the performance of these technologies should be compared to. Second, experimental work and modeling on those capture processes is discussed. The current state of patented CA immobilized based processes is also summarized. Finally, conclusions from both sides will be drawn and they will be connected to what has been exposed in the previous sections.

3.1. Gas absorption

3.1.1. Mass transfer theory

The classical in-series-resistance model shows that the overall mass transfer resistance is the sum of gas and liquid phase resistance. When the absorption includes chemical reaction, the liquid side individual mass transfer coefficient is modified by the enhancement factor, E [111]. The introduction of CA as free or immobilized has the objective of increasing E, in order to decrease the liquid phase resistance which is the dominant in the overall process [112] and directly affects to the needed surface contact area and the equipment size.

$$\frac{1}{K_G} = \frac{1}{k_g} + \frac{H}{Ek_l}$$

$$E = \frac{J,\ with\ chemical\ reaction}{J,\ without\ chemical\ reaction}\Big|_{equal\ driving\ force}$$

For 30%$_W$ MEA, the benchmark amine for CO_2 capture, large enhancement factors have been reported: ~440−150 (13%$_V$ CO_2, 0.1−0.3 CO_2/MEA mol) [113], ~96 (29.8%$_V$ CO_2, 0.45 CO_2/MEA mol) [114] or 82 (14%$_V$ CO_2, 10% loading) [115]. While aqueous solvents such as 30%$_W$ K_2CO_3 present much lower values: 1.2 (14%$_V$ CO_2,10% loading) [115] and 1.06 (1–1.5 bar CO_2) [116]. 0.5 M Na_2CO_3-$NaHCO_3$ also has a low enhancement factor of ~3.5 (0.52 bar CO_2) [117]. MDEA, a less energy intensive amine, shows better kinetics achieving around 20% of mass transfer performance of MEA [118] for the same concentration. The poor absorption rates described above are improved when CA is present as promoter. Experimental work in CA promoted K_2CO_3 solutions has yielded enhancement factors still lower than MEA, between 5.3–12 for a concentration range of 0.3−0.5 mg/mL CA [116,119,120]. Promisingly, simulations indicated that using a concentration of 10 mg/mL of CA would lead to a similar packed column height than 30%$_W$ MEA [112]. When promoted with 0.5 mg/mL of CA, Na_2CO_3 solutions can display an absorption rate increase by a factor 7.6 [120]. Modeling results also encourage the use of this solvent as the packing height could be reduced by a 24 factor when using CA 1 mg/mL in 0.3 M Na_2CO_3 compared to the unpromoted solvent [24]. A Pilot scale test with 3.5 mg/mL CA in MDEA showed a mass transfer equivalent to the 80% displayed by 30%$_w$ MEA. However, the stability of CA in MDEA can be more compromised than in carbonate solvents [119,120]. The enhancement factors provided by these solvents, although often significantly smaller than for MEA, are promising when all the benefits derived from lower reboiler duty and environmentally benign character are considered [11,13]. Previous discussed cases only focus on free CA which is generally the upper bound when immobilization is considered. How the three phases flue gas, solvent and solid catalyst are brought into contact has great importance to provide an enhancement factor as close as possible to the one obtained with free enzyme. The different configurations for post-combustion CO_2 capture based on immobilized CA enhanced absorption are described below.

3.1.2. Static devices: Packed-columns, scrubbers and bubble columns

While circulating through a packed column both phases, the flue gas and the solvent are brought into contact using a high surface packing material (Fig. 1). The goal of the packing is to ensure good contact between both phases and avoid phase coalescence. For bioaccelerated CO_2 capture, the column packing can be used as CA carrier. In order to determine the performance of this configuration, Iliuta and Iliuta [121] performed simulations. They modelled the CO_2 capture in a 4th generation random packing column with immobilized human CA II. The enzyme is immobilized in a porous layer (washcoat) coating the packing material. They concluded that diffusional mass transfer limitations around the packing and within the washcoat limits the enhancement compared to free enzyme. Increasing liquid velocity, enzyme loading and washcoat thickness reduction improves the performance. Experimental work has also shown these limitations. Leimbrink et al. [122,123] studied the absorption of CO_2 from a flue gas in a packed bed pilot plant using MDEA. Immobilized enzyme was in the form of beads introduced within a structured packing. Minors flux enhancements were observed compared to MDEA. Furthermore, when compared to free enzyme they were substantially lower. Additionally, Migliardini [124] investigated previously discussed polyurethane foam materials with covalent bounded CA as packing in a column to accelerate the absorption of CO_2 in water. Although they do not compare their results to free enzyme, they observed that the CO_2 conversion % was not enhanced very significantly unless a certain liquid flowrate was attained. Below this flowrate, mass transfer resistance within the liquid phase does not allow to fully exploit CA catalytic activity. Finally, Bhattacharya et al. [125] immobilized CA on the surface of a steel matrix (iron filings). The solvent (water) was sprayed to insure a thin liquid film covering the catalyst. They reported a large increment in CO_2 reduction when enzyme loading in the reactor was increased until a plateau is reached. For the given examples, it is clear that in order to effectively take advantage of the catalytic potential of CA i.e. to have an enhancement factor comparable to free enzyme, it is required to minimize the mass transfer resistance associated to the transfer of CO_2 from the interface to the enzyme active site. As it is schematized in Fig. 6C and it has been discussed in the theory section, when CA is dissolved the overall mass transfer resistance is the sum of the gas side and liquid side individual resistances. However, when CA is immobilized on/in the packing there are two other major contributors to consider that are external diffusion (liquid bulk to carrier surface, Fig. 6A and B) and internal diffusion

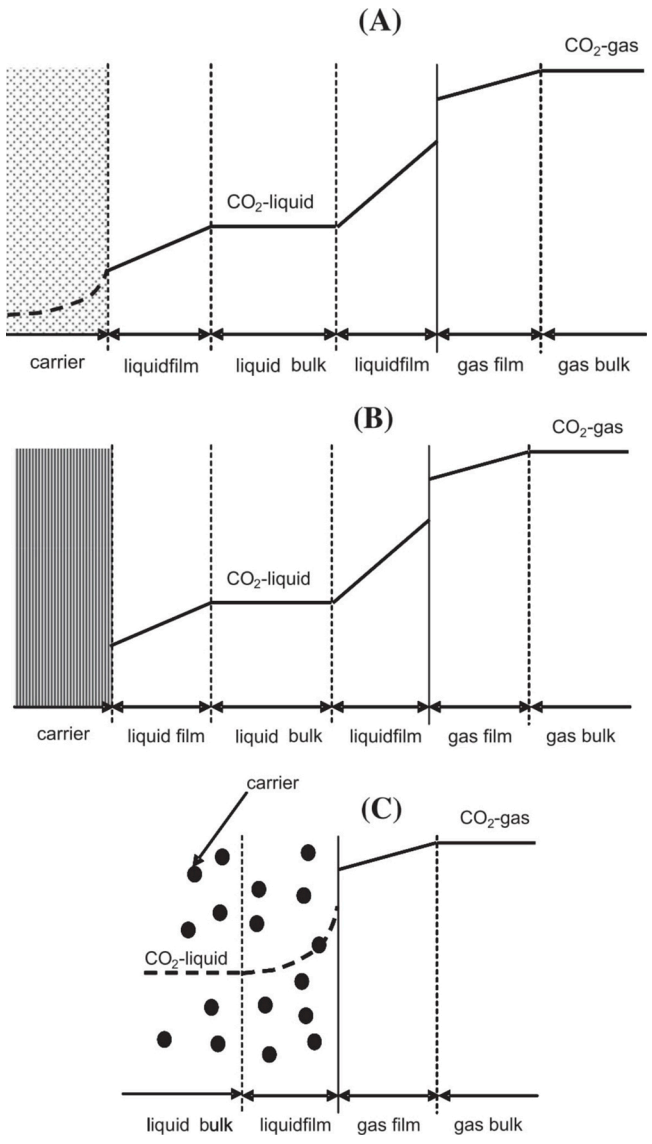

Fig. 6. CO_2 concentration profiles through different systems. From top to bottom: (A) CA is immobilized within a porous material that serves as packing, (B) CA is immobilized at the surface of a nonporous packing and (C) free CA is dissolved in the liquid phase or in the form of suspended immobilized enzyme in which the particle size is smaller than the thin film thickness. To simplify, non-catalyzed CO_2 hydration reaction within the liquid phase is neglected. Reprinted from [126] with the permission of Elsevier. Copyright (2012).

within the carrier (Fig. 6A). While the second one can be limited upon selection of an appropriate immobilization method and material, the first one is inherent to this configuration. When CA is immobilized on/in the support, CO_2 has to travel from the interface to the catalytic packing surface, a distance much larger than the liquid film thickness [24].

In order to improve mass transfer and fully exploit CA catalytic potential, instead of immobilizing the enzyme in/on the packing material, it can be immobilized in/on flowable microparticles that form a slurry. These particles will be homogenously distributed in the bulk liquid and in the thin liquid boundary layer next to the gas-liquid interface as these are designed to be smaller (Fig. 6A). The thin liquid film thickness depends on a number of factors, but it can be considered in the order of μm in size [24,127]. The use of flowable microparticles present better results from both experimental and simulation studies. Leimbrink et al. [128] prepared CA immobilized microparticles which were tested in the same set-up as before [122,123]. Here, absorption is accelerated by a factor 6 compared to MDEA and absorption rate is close to free enzyme.

With regards to modeling, Iliuta and Iliuta [129] simulated CO_2 absorption in a packed column where CA was immobilized on the packing and/or flowable microparticles. CO_2 removal was significantly increased by microparticles compared to packing immobilized CA, particularly when the later performance is limited by diffusion. When particle size is reduced absorption rates approach to free enzyme [24]. The use of microparticles, aiming to have an order of size close to the thin liquid film seems a promising alternative. Although the material has be selected to be compatible with the static packing to avoid fouling or blocking and to have a minimum mechanical strength.

Regarding industrial application, several patents from CO2 Solutions Inc. have been registered focused on CO_2 capture using immobilized CA and the configurations already discussed. Fradette et al. [130,120,131] described systems including an absorption and desorption units in which CO_2 is captured by a carbonate solution and it is regenerated in the stripper to obtain a CO_2 rich gas (Fig. 1a). CA can be in solution or immobilized on the packing material, for example on the surface of Raschig rings or in flowable microparticles such as nylon. A patent focused on microparticles smaller than liquid film thickness was published [132]. In addition, Penders et al. [133] developed an immobilized CA assisted desorption system. As CA accelerate both the direct and inverse reactions, both processes absorption and stripping can be favored. Blais and Rogers [134] developed a system in which CA is immobilized on non-porous particles. In this patent, the immobilisate is introduced in a packed bed reactor that improves the contact between the gas and liquid phase. The product, a bicarbonate rich solution, goes to an ion exchange system where bicarbonate is exchanged with hydroxyl ions or in another option is fed to a column where CA catalyze the CO_2 release using vacuum. As enzyme activity will decline over time, Madore et al. [135] patented an activity replenishment system in which the packing is put in contact with a replenish CA solution when required. Pilot demonstrations are important to prove a technology before going to the commercial scale. That's why the work by Bucholz et al. [136] is particularly interesting. They performed absorption tests in a ~8 m column containing structured packing with real flue gases from coal-fired power plan. They used as solvent potassium carbonate at 40 °C. Here, CA was entrapped inside a silica gel - PDMS coating of 200−300 μm covering the packing material surface. When CA was present, the mass transfer coefficient was enhanced by a factor 7 compared to non-catalyzed reaction and the system was able to capture 80% of CO_2. Demonstration continued during a 5 months period in which the mass transfer coefficient declined only about 20 %. Therefore, it is expected that it will take 1.5 years to reduce the performance up to the half. They reported foaming problems at the beginning because enzyme leaching. The application of free enzyme has to consider this challenge as well.

Other static configurations have received much less attention than packed columns. For example, the use of CA immobilized in scrubbers is scarce. Up to now, a CO2 Solutions Inc. patent by Fradette et al. [137] describes a spry tower in which the gas is introduced at the bottom and a liquid containing the biocatalyst is sprayed from the top using nozzles. The biocatalyst is either in solution or in the form of microparticles small enough to be ejected by the nozzles. Concerning bubble columns, Russo et al. [127] modelled a slurry bubble column where CA is free or in the form of fine particles. They concluded that the enhancements factors obtained using free CA in 20%$_W$ K_2CO_3 were limited by its solubility limit (0.1 mg/mL). The enhancement could be much larger when CA was in the form of microparticles as the apparent concentration can be increased beyond the solubility limit. This is not the case for CA immobilized on the packing surface as the total amount of enzyme that can immobilized is limited [119]. Finally, in a patent by Parent & Dutil [138] it is described a triphasic reactor in which enzyme immobilized in/on a support is maintained in suspension in an aqueous solvent.

3.1.3. *Dynamic devices*

Up to date, little attention in the literature has been dedicated to the

performance of such reactors. CO2 solutions proposed a more complex bioreactor design using the concept of process fluid dynamic intensification [139]. By using devices such as rotating bed reactors or rotating disk reactors large rotational speed leads to improved phase dispersion and reduced liquid film thickness. Thus, important improvements in mass transfer are obtained reducing the size of these equipment compared to conventional columns. Immobilizing enzymes can be a good opportunity to improve the resistance towards enzyme deactivation under such mechanical stresses and moving gas–liquid interfaces [140,141].

It should be noted that for the all the cases previously discussed, even if the performance of the immobilized is smaller than free enzyme, i.e. smaller enhancement factors, less enzyme is required when using immobilized. This is true when immobilized CA is the packing material or when flowable microparticles are continuously separated and recycled achieving a localized high apparent concentration. Using a given concentration of free enzyme implies to have that concentration throughout the liquid solvent in the entire installation.

3.1.4. Gas-liquid membrane contactors

A gas-liquid membrane contactor consists of a porous membrane placed between the gas and liquid phases. Membrane contactors haven been proposed as alternative to conventional packed columns because of their gas/liquid flow versatility, compactness and easy scale-up [142]. It has been argued that the presence of the membrane provided an additional resistance to the mass transfer. This is especially problematic when membrane wetting is present [143]. Nevertheless, the clear definition of gas-liquid interface provides an advantage in terms of CA immobilization because the enzyme can be placed at the gas-liquid interface or within the thin liquid film.

$$\frac{1}{K_G} = \frac{1}{k_g} + \frac{1}{k_m} + \frac{H}{Ek_l}$$

This has led to a large interest. Federspiel's group developed a series of CA immobilized hollow fiber membrane contactors to enhance CO_2 removal from blood. Although no linked to CO_2 capture, their results can be extrapolated to the use of hollow-fiber membrane contactors as CO_2 strippers. Among the membranes they used, firstly they studied surface modified poly(methyl pentene) to which CA was covalently attached [144,145]. Later, they developed amine propylene or poly(methyl pentene) membranes to with CA was covalently immobilized either directly or through a chitosan spacer being much more effective the later approach [146–148]. With regards to studies focused on post-combustion CO_2 removal, Yong et al. [116,149] prepared thin film composite membranes by in situ layer-by-layer assembling that were used to test the improvements in K_2CO_3 absorption kinetics in a hollow fiber contactor set-up. The deposited material was polyelectrolytes in which CA was adsorbed. Xu et al. [150] developed membranes with immobilized enzyme by modifying the surface of a PVDF hollow fiber membrane (polydopamine-polyethylenimine deposition) and investigated the improvements in CO_2 absorption comparing MEA and water. Finally, Hou et al. [151] fabricated a Janus membrane contactor having a layer of hydrophilic cross-linked carbon nanotubes on which CA was adsorbed. Later, the same authors [62] fabricated compose membranes by depositing CA covalently immobilized TiO_2 nanoparticles on top a PP porous membrane by a sol-gel coating method. These membranes were not tested in an absorption set-up. Nevertheless, they carried out experiments in which flowable CA covalently immobilized TiO_2 nanoparticles were used to promote the absorption in a membrane contactor [152]. All them, report significant improvements in CO_2 absorption rate, especially al lower liquid flowrates, indicating the advantage of placing CA at or near the interface. Once more, Iliuta & Iliuta [153] took the first steps in simulation in CO_2 capture using this configuration. They developed a modeling approach to membrane contactors in absorption in which CA was immobilized at the interface. They compared partial wetted and non-wetted pore mode of operation. Their results suggested that the use of enzyme immobilized membrane contactors is an interesting approach for improving the capture of CO_2. They pointed out that membrane wetting has a strong negative effect on the performance. When pore wetting is present, to have CA immobilized in the pores slightly reduces the overall mass transfer resistance but the detrimental effect of wetting is still very important. Finally, perhaps because of the novelty of gas-liquid membrane contactors, the number of patents describing membrane contactors with immobilized CA is reduced. Stolaroff et al. [154] presented a polymer membrane in which the enzyme was embedded within the polymer. The membrane separates the gas and liquid phase, therefore it can assimilated to a gas-liquid membrane contactor.

3.2. Gas permeation

In gas permeation, selective membranes are used to separate CO_2 from a gas mixture, see Fig. 7. The basic parameters to define the performance of this kind of membranes are permeability/permeance and selectivity. According to the Solution-Diffusion model [155], these parameters can be defined as:

$$P_{CO_2} = S_{CO_2} D_{CO_2}$$

$$\propto_{CO_2/N_2} = \frac{P_{CO_2}}{P_{N_2}}$$

While permeance and permeability are analogue to the mass transfer coefficient in gas absorption, membrane selectivity is equivalent to solvent selectivity. Highly permeable membranes are desired to obtain large CO_2 recovery and selective membranes are needed to attain high CO_2 purity in the permeate [156]. Achieving both targets is often difficult because of a trade-off between permeability and selectivity [157]. Comparison of MEA absorption and gas permeation, in terms of energy per ton of CO_2, yielded that in order to compete with MEA absorption, a selectivity of at least 100 is required for low CO_2 content flue gases (~10%) [158]. Once that a minimum selectivity is attained, the main membrane property controlling the cost is permeance. A Permeance of at least 1000 GPU (100 Barrer permeability for a 0.1 μm thick selective layer) is required to avoid huge membrane areas [159]. Extensive research has been carried out developing and testing different membranes to separate CO_2 from N_2 [160] including CA containing membranes. The advantage of immobilizing CA in a membrane used for gas permeation is the so-called Facilitated Transport Mechanism. As CO_2 is transformed into bicarbonate/carbonate, the net amount of CO_2 crossing the membrane is larger as it accounts for CO_2 gas (solution-diffusion mechanism) and ionized species (facilitated mechanism). As a consequence, the permeability of CO_2 and selectivity are increased.

Early examples of CA assisted selective membranes were focused on CO_2 separation from O_2 with the objective of air purification in confined spaces. They consisted of a small volume of CA aqueous solution entrapped within the pores of a porous membrane by capillary force (supported liquid membranes) [161,162], see Table 2. As water or aqueous solutions have low viscosity, large permeabilites were

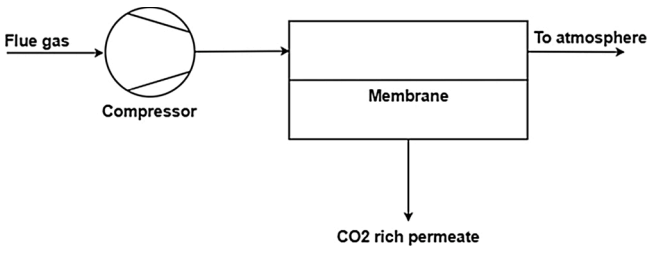

Fig. 7. Basic elements in a gas separation unit. Note that these membranes are selective while those in gas-liquid membrane contactors are not.

Table 2
Carbonic anhydrase promoted selective membranes.

Membrane type	Permeability	Selectivity	Comments	Ref
Supported liquid membranes				
	~53.73 GPU, ~3761 Barrer (70 μm), 6 fold		Concentrated K_2CO_3 (2 M). After some days, no improvement is observed. CO_2 – O_2 separation, 5% CO_2.	[161]
	~53.73 GPU, 10 fold (flux)	250	1 M $NaHCO_3$. CO_2-O_2 separation.	[162]
	2500 GPU	788	Ultra-thin liquid membrane. Buffer. 3 – month stability at ambient conditions.	[163, 164]
	4.2×10^{-7} cm^2/s, 20 % improvement	~37	[BMIm][NTf2] ionic liquid. Enzyme loading 0.01 $\%_w$. 0.753 water activity.	[165]
	4.36×10^{-6} cm^2/s, 2.2 fold	30.28	[BMIm][NTf2] ionic liquid, spinach leaf CA. 4 Weeks stability. Loading ~ 0.35 $\%_w$.	[167]
	734 Barrer (373 K, 0.025 $\%_w$ CA), 40 % improvement	36 (373 K, 0.025 $\%_w$ CA)	[BMIm][NTf2] ionic liquid, thermoresistant CA. Test at different temperatures and loadings. Water activity 0.836.	[166]
	142.17 Barrer, 60 % improvement	79.91, 67 % improvement	Choline chloride-urea (1:2), 0.1 mg/mL CA.	[169]
Sandwiched liquid membranes				
	430 GPU, 141,900 Barrer (330 μm liquid membrane)	1400	Phosphate buffer. 0.1 % CO_2 in the feed. 30 °C.	[172]
	141 GPU, 46,530 Barrer (330 μm liquid membrane)	1090	Phosphate buffer. 0.1 % CO_2 in the feed. 30 °C.	[173]
	14.4 GPU (~6 fold), 216 Barrer (15 μm thin film)	28.7	CO_2 – He separation (80% CO_2). 40 °C. 80% RH feed gas. Sprayed liquid membrane covered by a dense film.	[174]
Liquid/hydrogel interstitially entrapped hollow-fiber membranes				
	~92 GPU	~234	1 M $NaHCO_3$, 3 mg/mL CA. 10%CO_2.	[175]
	49.25 GPU	820	Poly(acrylic acid-co-acrylamide)/ hydrotalcite hydrogels. 0.1 % CO_2.	[176]
Thin-film composite membranes				
	24.16 GPU, ~96 barrer (4 μm), 3.2 fold	168.8, 20.9 fold	CA immobilized on ZIF – 8 MOFs. Stable operation during at least 40 h.	[178]
	~48 GPU, 0.65 fold	58, 1.4 fold	CA dispersed in polyvinyl alcohol. Humidified gas, 15 $\%_v$ CO_2.	[179]
	~52 GPU, 1.27 fold	74, 10.5 fold	Vinyl modified CA – acrylamide copolymer, Humidified gas, 5$\%_v$ CO_2.	[179]

observed. In fact, the theoretical CO_2 permeability in pure water is 2100 barrer [161]. However, the main disadvantage of supported liquid membranes is the inherent lack of liquid membrane stability. Mechanical removal by transmembrane pressure differences and evaporation are the main threats. Recently, Fu et al. [163,164] made an outstanding contribution by developing membranes with immobilized CA in a pore contained ultra-thin water film. The supported liquid film was small enough to contain roughly 2 molecules of CA increasing by a factor 10 the achievable CA concentration in solution and making CA catalysis the rate limiting step. Because nanoconfinement, the liquid membrane was expected to be much more stable. Other efforts in the direction of limiting liquid membrane evaporation focused on supported ionic liquid membranes [165–167]. So far, all of them have been focused on the hydrophobic ionic liquid [BMIm][NTf2]. A certain water activity (humidity in the liquid membrane) was required to display enhancements in permeability although reducing selectivity compared to dry ionic liquid. Later, Nemestóthy et al. [168] showed that a large percentage of enzyme was denatured by contact with the hydrophobic ionic liquid. This means that a very small amount of enzyme could improve significantly the performance. Recently, supported liquid membranes containing deep eutectic solvents with solubilized CA have also been analyzed [169, 170]. It was indicated that DES low pH could have a negative effect in the enzyme. In any case, industrial application of supported liquid membranes has to overcome the lack of liquid membrane mechanical stability [171]. Some authors have suggested to entrap the CA dissolved liquid membrane between porous membranes. This can be performed either by sandwiching the liquid membrane between two flat sheet porous membranes [172–174] or by placing it in the interstitial space of two arrays of hollow fibers [175]. Such configurations allow continuous supply of fresh CA solution to overcome evaporation. Furthermore, they can withstand a much larger pressure difference than supported liquid membranes [175]. Concerning their performance, attention must be paid to the size of the liquid membrane. Important reduction in permeance will be observed if the diffusion distance is increased. On top of that, pore wetting of the porous membranes between which the liquid membrane is entrapped would increase substantially the mass transfer resistance. Previously reported configurations does not, in principle, improve the stability of the enzyme as true immobilization does. Instead of using CA in free solution, some authors have immobilized CA in hydrogels and have placed them in the interstitial space of a hollow fiber set [176,177]. Since the enzyme is not suggested to leaching, highly porous and hydrophilic hydrogels can be used. Apart from the cited examples, so far, the replacement of the CA containing liquid membrane by a humidified solid or gel-like carriers remains largely unexplored. Probably because the lower diffusivities compared to liquid materials. Finally, taking into account that CA activity is hindered by diffusional limitations its immobilization in materials shaped in the form of mechanical stable thin films (nm order) such as thin film composite membranes can be a tentative election. In this regard, Zhang et al. [178] have provided interesting results testing composite membranes in which the selective layer is made of CA immobilized ZIF-8 MOFs. CA presence enhance both permeability and selectivity. However, reported permeability is not competitive enough. Concerning the state of patents, in a patent by Sandru [179], the invention is focused on polymeric membranes having a selective polymeric layer in which CA has been immobilized. Here it is discussed that the select permeable polymer has to be hydrophilic and/or permeable to water vapor to allow enzyme hydration. CA can be immobilized in a variety of ways including entrapment within a casted film made from an aqueous soluble polymer, enzyme modification to include vinyl groups and subsequent copolymerization or covalent bonding at the surface. Surprisingly, some reported results indicate that although improving selectivity, CA presence can reduce membrane permeability. Their performance was stable during at least 12 days.

4. Conclusions regarding the industrial implementation of immobilized carbonic anhydrase

The number of recent publications in CA application for CO_2 capture reflects the growing interest in this biocatalyst [19,180,181]. Many of the studies concerning CA deal with immobilization aiming to overcome the issues related to the use of free enzyme. Different CAs have been immobilized in a variety of materials and following different methodologies. Although some general trends can be drawn from results presented in Table 1, fair comparisons are difficult. An additional challenge is to implement these carriers in an appropriate industrial configuration in order to fully exploit CA properties to achieve a promising CO_2 separation technology. To bring together laboratory developed heterogeneous biocatalysts and industrially relevant CO_2 separation technologies three core issues need to be addressed: Long-term operational stability, equipment size and environmental impact.

4.1. Long-term operational stability and its effect on the OPEX

For an amine-based absorption installation the average replacement rate is about 1 kg of amine per ton of CO_2 captured and MEA price is 1.3 $/kg [182]. Even if a significantly lower CA concentration, less than 1% w, is required to compete with 30%$_W$ MEA, CA price can be much higher. Commercially purified CA from bovine erythrocytes (blood) costs 1.25 $/mg [183]. However, to produce CA at a larger scale is more suitable to use genetically modified organisms such as recombinant *Escherichia coli* [184,185]. The price of an industrially produced enzyme will strongly depend on a variety of factors including production volume, fermentation yield and the required purification degree [186]. Considering these variables the price of an enzyme can be estimated to be between hundred and several thousands $/kg [186]. Nevertheless, some industrial enzymes present lower prices (10–20 $/kg) [187,188]. Interestingly, in a recently published techno-economical analysis, free CA accounted for the 7.3% of OPEX and 4.6% of the total annual cost in a CA promoted potassium carbonate CO_2 absorption system [189]. The authors used a price of 480 $/kg in their analysis. Low CA replacement rate or make-up (kg CA/ton CO_2) is thus required to decrease the OPEX. Good thermal stability in the range of temperatures commonly present in CO_2 separation and resilience to the solvent and flue gases impurities are therefore necessary. Using CA varieties from thermophilic organisms can potentially solve this issue. However, even thermophilic CA present a shelf life period, which is shortened at higher temperatures [190]. An appropriate enzyme immobilization protocol can remarkably increase enzyme stability. Therefore, the most promising choice for a long-term thermal stability is the combination of a thermally stable enzyme variety and a suitable immobilization matrix. Immobilization generally improves stability towards the solvent and flue gases impurities as well. It is important to realize that, although reducing CA make-up, enzyme immobilization can increase the biocatalyst price by a significant factor. A simple immobilization procedure such as adsorption can increase the specific enzyme price by 4 [186]. Such factor is derived from the cost associated to the immobilization process (raw materials, equipment, etc.) and it strongly depends on the carrier price, especially for cheap enzymes [186].

4.2. Equipment size and its effect on the CAPEX

Large mass transfer coefficients provide a reduction in equipment size, e.i. CAPEX that can be an important contributor to the overall cost. So far, reported values of free CA enhancement factors are smaller than for MEA. That is why it is required to use highly active CA varieties and high concentrations. First, using immobilized enzymes, the apparent concentration of enzyme can be larger than the solubility limit. Second, the new CA immobilized MOFs and nanoflowers materials have shown unprecedented activity enhancements overcoming the upper bound imposed by free enzyme. That is why the combination of both strategies might yield enhancement factors closer or superior to the benchmark solvent. In order to fully exploit the efficiency of immobilized enzyme it has to be close to the interface. The use of gas-liquid membrane contactors or absorption with suspended microparticles could be interesting although each present challenges. Membrane wetting could endanger the long-term performance of the absorption equipment while nanostructured materials are fragile and therefore it is not convenient to use them in the form of suspended microparticles. Their inclusion in more flexible and resistant materials would enhance their mechanical stability but compromising their performance. Finally, regarding to the use of immobilized enzymes in gas permeation membranes, except a few cases, their performance is not competitive enough compared to benchmark membranes in gas separation. Nevertheless, studies focused on true CA immobilization within these membranes remain scarce and further research is required

4.3. Environmental impact

As the final goal is CO_2 emission mitigation, despite of being less powerful than amines, the use of more benign solvents is promising accounting for their lower environmental impact and lower heat of regeneration. CA fabrication and enzyme make-up does not have an important influence in the CO_2 absorption process environment impacts [191]. The effect of immobilization protocol, however, remains unexplored. In this regard, the use of natural carriers and simple immobilization procedures no requiring the use of toxic chemicals might be preferred.

So far, CA assisted absorption seems more promising than CA enhanced selective membranes, although the later technology has received less attention and more research is required. Concerning absorption, the use of low reboiler duty environmentally benign solvents promoted by CA is a promising alternative to the benchmark process considering their lower environmental impact and lower cost per ton of CO_2 [189]. A number of industrial projects in recent years proves the attractiveness of the concept [19]. However, the high price of CA and its limited stability in harsh conditions have been repeatedly highlighted as the mayor limitations to its industrial implementation [18,81,181,184,192,193]. Nevertheless, more economic and environmental studies performing a side by side comparison to absorption using amines are required in order to truly evaluate the suitability of CA promoted CO_2 capture processes. In those studies, it is crucial to assess the effect of CA cost, activity and stability in its applicability. Immobilization is expected to play an important role in CA industrial implementation, therefore, future economic/environmental studies should consider the effect of immobilization in the final biocatalyst cost, activity and stability. The comparison of different immobilization methods would be interesting. Finally, the development of new carriers providing unprecedented improvements in CA activity and stability may foster the application of CA at industrial scale. In order to provide more conclusive results, they should be studied in conditions relevant for post combustion CO_2 capture and tested in appropriate configurations.

Declaration of Competing Interest

The authors report no declarations of interest.

Acknowledgements

The authors are grateful for the funding provided by the European Research Council. Such funding was received from the European Union's Horizon 2020 Research and Innovation Programme (Grant Agreement ERC Starting Grant UE H2020 CO2LIFE 759630).

References

[1] International Energy Outlook 2019 With Projections to 2050, 85, U.S. Energy Inf. Adm. (EIA), Off. Energy Anal. Washington, DC, 2019.

[2] IEA. Data & Statistics - IEA. International energy agency Available at: https://www.iea.org/data-and-statistics/?country=WORLD&fuel=CO2 emissions&indicator=CO2 emissions by sector. (Accessed: 28 May 2020).

[3] E.I. Koytsoumpa, C. Bergins, E. Kakaras, The CO_2 economy: review of CO_2 capture and reuse technologies, J. Supercrit. Fluids 132 (2018) 3–16.

[4] L.N. He, J.Q. Wang, J.L. Wang, Carbon dioxide chemistry: examples and challenges in chemical utilization of carbon dioxide, Pure Appl. Chem. 81 (2009) 2069–2080.

[5] Y. Artanto, et al., Performance of MEA and amine-blends in the CSIRO PCC pilot plant at Loy Yang Power in Australia, Fuel 101 (2012) 264–275.

[6] E. Favre, Membrane processes and postcombustion carbon dioxide capture: challenges and prospects, Chem. Eng. J. 171 (2011) 782–793.

[7] D.Y.C. Leung, G. Caramanna, M.M. Maroto-Valer, An overview of current status of carbon dioxide capture and storage technologies, Renew. Sustain. Energy Rev. 39 (2014) 426–443.

[8] S. Mokhatab, W.A. Poe, J.Y. Mak, Natural gas treating. Handbook of Natural Gas Transmission and Processing, Elsevier, 2019, pp. 231–269, https://doi.org/10.1016/b978-0-12-815817-3.00007-1.

[9] P. Luis, Use of monoethanolamine (MEA) for CO_2 capture in a global scenario: consequences and alternatives, Desalination 380 (2016) 93–99.

[10] T. Nguyen, M. Hilliard, G.T. Rochelle, Amine volatility in CO_2 capture, Int. J. Greenh. Gas Control 4 (2010) 707–715.

[11] T. Grant, C. Anderson, B. Hooper, Comparative life cycle assessment of potassium carbonate and monoethanolamine solvents for CO_2 capture from post combustion flue gases, Int. J. Greenh. Gas Control 28 (2014) 35–44.

[12] A.J. Reynolds, T.V. Verheyen, S.B. Adeloju, E. Meuleman, P. Feron, Towards commercial scale postcombustion capture of CO_2 with monoethanolamine solvent: key considerations for solvent management and environmental impacts, Environ. Sci. Technol. 46 (2012) 3643–3654.

[13] M. Bui, et al., Carbon capture and storage (CCS): the way forward, Energy Environ. Sci. 11 (2018) 1062–1176.

[14] K. Stéphenne, Start-up of world's first commercial post-combustion coal fired ccs project: contribution of shell cansolv to saskpower boundary dam iccs project, Energy Procedia 63 (2014) 6106–6110. Elsevier Ltd.

[15] D.M. Kern, The hydration of carbon dioxide, J. Chem. Educ. 37 (1960) 14–23.

[16] K.S. Smith, C. Jakubzick, T.S. Whittam, J.G. Ferry, Carbonic anhydrase is an ancient enzyme widespread in prokaryotes, Proc. Natl. Acad. Sci. USA 96 (1999) 15184–15189.

[17] S. Lindskog, Structure and mechanism of carbonic anhydrase, Pharmacol. Ther. 74 (1997) 1–20.

[18] A. Nocentini, M. Tanc, CO_2-capture by engineered mammalian carbonic anhydrases. Carbonic Anhydrases: Biochemistry and Pharmacology of an Evergreen Pharmaceutical Target, Elsevier, 2019, pp. 515–530, https://doi.org/10.1016/B978-0-12-816476-1.00023-X.

[19] T. Sharma, S. Sharma, H. Kamyab, A. Kumar, Energizing the CO_2 utilization by chemo-enzymatic approaches and potentiality of carbonic anhydrases: a review, J. Clean. Prod. 247 (2020).

[20] Voyer, N., Daigle, R., Madore, É. & Fradette, S. Co2 capture methods using thermovibrio ammonificans carbonic anhydrase. U.S. Pat. No. 9,968,885 (2018).

[21] J. Hou, et al., Accelerated CO_2 hydration with thermostable Sulfurihydrogenibium azorense carbonic anhydrase-chitin binding domain fusion protein immobilised on chitin support, Int. J. Mol. Sci. 20 (2019).

[22] G. Hu, et al., Enzymatic carbon dioxide capture using a thermally stable carbonic anhydrase as a promoter in potassium carbonate solvents, Chem. Eng. J. 307 (2017) 49–55.

[23] S. Zhang, Z. Zhang, Y. Lu, M. Rostam-Abadi, A. Jones, Activity and stability of immobilized carbonic anhydrase for promoting CO_2 absorption into a carbonate solution for post-combustion CO_2 capture, Bioresour. Technol. 102 (2011) 10194–10201.

[24] N.J.M.C. Penders-van Elk, et al., Kinetics of absorption of carbon dioxide in aqueous amine and carbonate solutions with carbonic anhydrase, Int. J. Greenh. Gas Control 12 (2013) 259–268.

[25] J.R. Collett, R.W. Heck, A.J. Zwoster, Dissolved carbonic anhydrase for enhancing post-combustion carbon dioxide hydration in aqueous ammonia, Energy Procedia 4 (2011) 240–244. Elsevier Ltd.

[26] R.A. Sheldon, S. van Pelt, Enzyme immobilisation in biocatalysis: why, what and how, Chem. Soc. Rev. 42 (2013) 6223–6235.

[27] W. Tischer, F. Wedekind, Immobilized Enzymes: Methods and Applications, 1999, pp. 95–126, https://doi.org/10.1007/3-540-68116-7_4.

[28] N.U. Meldrum, F.J.W. Roughton, Carbonic anhydrase. Its preparation and properties, J. Physiol. 80 (1933) 113–142.

[29] A. Basso, S. Serban, Industrial applications of immobilized enzymes—a review, Mol. Catal. 479 (2019) 110607.

[30] I. Eş, J.D.G. Vieira, A.C. Amaral, Principles, techniques, and applications of biocatalyst immobilization for industrial application, Appl. Microbiol. Biotechnol. 99 (2015) 2065–2082.

[31] L. Goldstein, [29] kinetic behavior of immobilized enzyme systems, Methods Enzymol. 44 (1976) 397–443.

[32] F. Secundo, Conformational changes of enzymes upon immobilisation, Chem. Soc. Rev. 42 (2013) 6250–6261.

[33] M. Hartmann, X. Kostrov, Immobilization of enzymes on porous silicas – benefits and challenges, Chem. Soc. Rev. 42 (2013) 6277–6289.

[34] Q. Liu, et al., User-tailored metal-organic frameworks as supports for carbonic anhydrase, ACS Appl. Mater. Interfaces 10 (2018) 41326–41337.

[35] P. Shao, H. Chen, Q. Ying, S. Zhang, Structure-activity relationship of carbonic anhydrase enzyme immobilized on various silica-based mesoporous molecular sieves for CO2 absorption into a potassium carbonate solution, Energy Fuels 34 (2020) 2089–2096.

[36] H.P. Khameneh, et al., A spectroscopic study on the absorption of carbonic anhydrase onto the nanoporous silica nanoparticle, Int. J. Biol. Macromol. 99 (2017) 739–745.

[37] J.K. Kim, M.A.A. Abdelhamid, S.P. Pack, Direct immobilization and recovery of recombinant proteins from cell lysates by using EctP1-peptide as a short fusion tag for silica and titania supports, Int. J. Biol. Macromol. 135 (2019) 969–977.

[38] R. Yadav, et al., Immobilization of carbonic anhydrase on chitosan stabilized Iron nanoparticles for the carbonation reaction, Water Air Soil Pollut. 223 (2012) 5345–5356.

[39] S. Wanjari, C. Prabhu, T. Satyanarayana, A. Vinu, S. Rayalu, Immobilization of carbonic anhydrase on mesoporous aluminosilicate for carbonation reaction, Microporous Mesoporous Mater. 160 (2012) 151–158.

[40] M. Vinoba, M. Bhagiyalakshmi, S.K. Jeong, Y.I.I. Yoon, S.C. Nam, Immobilization of carbonic anhydrase on spherical SBA-15 for hydration and sequestration of CO_2, Colloids Surf. B Biointerfaces 90 (2012) 91–96.

[41] M. Vinoba, M. Bhagiyalakshmi, S.K. Jeong, Y.I. Yoon, S.C. Nam, Carbonic anhydrase conjugated to nanosilver immobilized onto mesoporous SBA-15 for sequestration of CO_2, J. Mol. Catal. B Enzym. 75 (2012) 60–67.

[42] M. Vinoba, K.S. Lim, S.K. Lee, S.K. Jeong, M. Alagar, Immobilization of human carbonic anhydrase on gold nanoparticles assembled onto amine/thiol-functionalized mesoporous SBA-15 for biomimetic sequestration of CO2, Langmuir 27 (2011) 6227–6234.

[43] A. Rimola, M. Sodupe, P. Ugliengo, Affinity scale for the interaction of amino acids with silica surfaces, J. Phys. Chem. C 113 (2009) 5741–5750.

[44] S. Hosseinkhani, M. Nemat-Gorgani, Partial unfolding of carbonic anhydrase provides a method for its immobilization on hydrophobic adsorbents and protects it against irreversible thermoinactivation, Enzyme Microb. Technol. 33 (2003) 179–184.

[45] S. Wanjari, et al., Immobilization of carbonic anhydrase on chitosan beads for enhanced carbonation reaction, Process Biochem. 46 (2011) 1010–1018.

[46] C. Prabhu, et al., Immobilization of carbonic anhydrase enriched microorganism on biopolymer based materials, J. Mol. Catal. B Enzym. 60 (2009) 13–21.

[47] A. Sharma, A. Bhattacharya, A. Shrivastava, Biomimetic CO_2 sequestration using purified carbonic anhydrase from indigenous bacterial strains immobilized on biopolymeric materials, Enzyme Microb. Technol. 48 (2011) 416–426.

[48] C. Prabhu, et al., Carbon composite beads for immobilization of carbonic anhydrase, J. Mol. Catal. B Enzym. 71 (2011) 71–78.

[49] F.A. Simsek-Ege, G.M. Bond, J. Stringer, Polyelectrolyte cages for a novel biomimetic CO2 sequestration system. Environ. Challenges Greenh. Gas Control Foss. Fuel Util. 21st Century, 2002, pp. 133–145, https://doi.org/10.1007/978-1-4615-0773-4_10.

[50] S. Wanjari, C. Prabhu, N. Labhsetwar, S. Rayalu, Biomimetic carbon dioxide sequestration using immobilized bio-composite materials, J. Mol. Catal. B Enzym. 93 (2013) 15–22.

[51] C. Mateo, J.M. Palomo, G. Fernandez-Lorente, J.M. Guisan, R. Fernandez-Lafuente, Improvement of enzyme activity, stability and selectivity via immobilization techniques, Enzyme Microb. Technol. 40 (2007) 1451–1463.

[52] M. Vinoba, M. Bhagiyalakshmi, S.K. Jeong, Y.I. Yoon, S.C. Nam, Capture and sequestration of CO_2 by human carbonic anhydrase covalently immobilized onto amine-functionalized SBA-15, J. Phys. Chem. C 115 (2011) 20209–20216.

[53] S. Bhattacharya, M. Schiavone, S. Chakrabarti, S.K. Bhattacharya, CO_2 hydration by immobilized carbonic anhydrase, Biotechnol. Appl. Biochem. 38 (2003) 111.

[54] P.C. Sahoo, et al., Accelerated CO_2 capture in hybrid solvent using co-immobilized enzyme/complex on a hetero-functionalized support, J. CO2 Util. 21 (2017) 77–81.

[55] H.K. Lim, D.R. Kim, I.T. Hwang, Sequestration of CO2 into $CaCO_3$ using carbonic anhydrase immobilization on functionalized aluminum oxide, Appl. Biochem. Microbiol. 55 (2019) 375–379.

[56] J. Sun, L. Wei, Y. Wang, Z. Zhao, W. Liu, Immobilization of carbonic anhydrase on polyvinylidene fluoride membranes, Biotechnol. Appl. Biochem. 65 (2018) 362–371.

[57] J. Sun, C. Wang, Y. Wang, S. Ji, W. Liu, Immobilization of carbonic anhydrase on polyethylenimine/dopamine codeposited membranes, J. Appl. Polym. Sci. 136 (2019) 47784.

[58] G. Merle, S. Fradette, E. Madore, J.E. Barralet, Electropolymerized carbonic anhydrase immobilization for carbon dioxide capture, Langmuir 30 (2014) 6915–6919.

[59] S.V. Rao, K.W. Anderson, L.G. Bachas, Oriented immobilization of proteins, Mikrochim. Acta 128 (1998) 127–143.

[60] S. Zhang, Y. Lu, X. Ye, Catalytic behavior of carbonic anhydrase enzyme immobilized onto nonporous silica nanoparticles for enhancing CO_2 absorption into a carbonate solution, Int. J. Greenh. Gas Control 13 (2013) 17–25.

[61] P. Wang, Nanoscale biocatalyst systems, Curr. Opin. Biotechnol. 17 (2006) 574–579.

[62] J. Hou, G. Dong, B. Xiao, C. Malassigne, V. Chen, Preparation of titania based biocatalytic nanoparticles and membranes for CO_2 conversion, J. Mater. Chem. A Mater. Energy Sustain. 3 (2015) 3332–3342.

[63] M. Lundqvist, I. Sethson, B.H. Jonsson, Protein adsorption onto silica nanoparticles: conformational changes depend on the particles' curvature and the protein stability, Langmuir 20 (2004) 10639–10647.

[64] G. Jing, F. Pan, B. Lv, Z. Zhou, Immobilization of carbonic anhydrase on epoxy-functionalized magnetic polymer microspheres for CO_2 capture, Process Biochem. 50 (2015) 2234–2241.
[65] S. Faridi, H. Bose, T. Satyanarayana, Utility of immobilized recombinant carbonic anhydrase of Bacillus halodurans TSLV1 on the surface of modified Iron Magnetic nanoparticles in carbon sequestration, Energy Fuels 31 (2017) 3002–3009.
[66] S. Peirce, et al., Kinetic characterization of carbonic anhydrase immobilized on magnetic nanoparticles as biocatalyst for CO_2 capture, Biochem. Eng. J. 138 (2018) 1–11.
[67] A.H.A. Al-Dhrub, S. Sahin, I. Ozmen, E. Tunca, M. Bulbul, Immobilization and characterization of human carbonic anhydrase I on amine functionalized magnetic nanoparticles, Process Biochem. 57 (2017) 95–104.
[68] R. Perfetto, et al., Production and covalent immobilisation of the recombinant bacterial carbonic anhydrase (SspCA) onto magnetic nanoparticles, J. Enzyme Inhib. Med. Chem. 32 (2017) 759–766.
[69] S.S.W. Effendi, C.Y. Chiu, Y.K. Chang, I.S. Ng, Crosslinked on novel nanofibers with thermophilic carbonic anhydrase for carbon dioxide sequestration, Int. J. Biol. Macromol. (2019), https://doi.org/10.1016/j.ijbiomac.2019.11.234.
[70] T. Takigawa, Y. Endo, Effects of glutaraldehyde exposure on human health, J. Occup. Health 48 (2006) 75–87.
[71] S.H. Jun, et al., Stabilized and immobilized carbonic anhydrase on electrospun nanofibers for enzymatic CO2 conversion and utilization in expedited microalgal growth, Environ. Sci. Technol. 54 (2020) 1223–1231.
[72] J.D. Cui, S.R. Jia, Optimization protocols and improved strategies of cross-linked enzyme aggregates technology: current development and future challenges, Crit. Rev. Biotechnol. 35 (2015) 15–28.
[73] S. Peirce, et al., Structure and activity of magnetic cross-linked enzyme aggregates of bovine carbonic anhydrase as promoters of enzymatic CO_2 capture, Biochem. Eng. J. 127 (2017) 188–195.
[74] S. Peirce, et al., Immobilization of carbonic anhydrase for biomimetic CO_2 capture in a slurry absorber as cross-linked enzyme aggregates (CLEA), Chem. Eng. Trans. 43 (2015) 259–264.
[75] D.Y. Xu, Y. Yang, Z. Yang, Activity and stability of cross-linked tyrosinase aggregates in aqueous and nonaqueous media, J. Biotechnol. 152 (2011) 30–36.
[76] J.M. Park, et al., Immobilization of lysozyme-CLEA onto electrospun chitosan nanofiber for effective antibacterial applications, Int. J. Biol. Macromol. 54 (2013) 37–43.
[77] J. Li, et al., Investigation on the immobilization of carbonic anhydrase and the catalytic absorption of carbon dioxide, Energy Fuels 31 (2017) 778–784.
[78] E. Ozdemir, Biomimetic CO_2 sequestration: 1. Immobilization of carbonic anhydrase within polyurethane foam, Energy Fuels 23 (2009) 5725–5730.
[79] Y. Han, et al., Silk fibroin-based hydrogels as a protective matrix for stabilization of enzymes against pH denaturation, Mol. Catal. 457 (2018) 24–32.
[80] B. Kaczmarek, K. Nadolna, A. Owczarek, The physical and chemical properties of hydrogels based on natural polymers. Hydrogels Based on Natural Polymers, Elsevier, 2019, pp. 151–172, https://doi.org/10.1016/B978-0-12-816421-1.00006-9.
[81] R.R. Yadav, et al., Immobilization of carbonic anhydrase in alginate and its influence on transformation of CO_2 to calcite, Process Biochem. 47 (2012) 585–590.
[82] Y. Zhu, W. Li, G. Sun, Q. Tang, H. Bian, Enzymatic properties of immobilized carbonic anhydrase and the biocatalyst for promoting CO_2 capture in vertical reactor, Int. J. Greenh. Gas Control 49 (2016) 290–296.
[83] F.A. Simsek-Ege, G.M. Bond, J. Stringer, A biomimetic route to environmentally friendly CO2 sequestration: catalyst immobilization, in: The Global Climate Change: A Coordinated Response by Electrochemistry and Solid-State Science and Technology, 162, 2001.
[84] F.A. Simsek-Ege, G.M. Bond, J. Stringer, Matrix molecular weight cut-off for encapsulation of carbonic anhydrase in polyelectrolyte beads, J. Biomater. Sci. Polym. Ed. 13 (2002) 1175–1187.
[85] Y.T. Zhang, et al., Synthesis and characterization of poly(acrylic acid-co-acrylamide)/ hydrotalcite nanocomposite hydrogels for carbonic anhydrase immobilization, J. Polym. Sci. Part A 47 (2009) 3232–3240.
[86] Y.T. Zhang, T.T. Zhi, L. Zhang, H. Huang, H.L. Chen, Immobilization of carbonic anhydrase by embedding and covalent coupling into nanocomposite hydrogel containing hydrotalcite, Polymer 50 (2009) 5693–5700.
[87] B. Ekman, I. Sjöholm, Improved stability of proteins immobilized in microparticles prepared by a modified emulsion polymerization technique, J. Pharm. Sci. 67 (1978) 693–696.
[88] P. Edman, B. Ekman, I. Sjöholm, Immobilization of proteins in microspheres of biodegradable polyacryldextran, J. Pharm. Sci. 69 (1980) 838–842.
[89] J.D. Badjić, N.M. Kostić, Effects of encapsulation in sol-gel silica glass on esterase activity, conformational stability, and unfolding of bovine carbonic anhydrase II, Chem. Mater. 11 (1999) 3671–3679.
[90] C. Forsyth, T.W.S. Yip, S.V. Patwardhan, CO_2 sequestration by enzyme immobilized onto bioinspired silica, Chem. Commun. 49 (2013) 3191–3193.
[91] N. Favre, Y. Ahmad, A.C. Pierre, Biomaterials obtained by gelation of silica precursor with CO_2 saturated water containing a carbonic anhydrase enzyme, J. Sol-Gel Sci. Technol. 58 (2011) 442–451.
[92] H. Furukawa, K.E. Cordova, M. O'Keeffe, O.M. Yaghi, The chemistry and applications of metal-organic frameworks, Science 341 (2013) 974.
[93] X. Lian, et al., Enzyme-MOF (metal-organic framework) composites, Chem. Soc. Rev. 46 (2017) 3386–3401.
[94] S. Zhang, et al., Carbonic anhydrase Enzyme-MOFs composite with a superior catalytic performance to promote CO 2 absorption into tertiary amine solution, Environ. Sci. Technol. 52 (2018) 12708–12716.
[95] V. Asadi, et al., Novel bovine carbonic anhydrase encapsulated in a metal-organic framework: a new platform for biomimetic sequestration of CO_2, RSC Adv. 9 (2019) 28460–28469.
[96] S. Ren, et al., Carbonic Anhydrase@ZIF-8 hydrogel composite membrane with improved recycling and stability for efficient CO_2 capture, J. Agric. Food Chem. 67 (2019) 3372–3379.
[97] S. Ren, et al., Immobilized carbonic anhydrase on mesoporous cruciate flower-like metal organic framework for promoting CO_2 sequestration, Int. J. Biol. Macromol. 117 (2018) 189–198.
[98] M. Jiao, et al., Fast immobilization of human carbonic anhydrase II on Ni-Based metal-organic framework nanorods with high catalytic performance, Catalysts 10 (2020) 401.
[99] Y. Zhang, J. Ge, Z. Liu, Enhanced activity of immobilized or chemically modified enzymes, ACS Catal. 5 (2015) 4503–4513.
[100] E. Gkaniatsou, et al., Metal-organic frameworks: a novel host platform for enzymatic catalysis and detection, Mater. Horiz. 4 (2017) 55–63.
[101] J. Ge, J. Lei, R.N. Zare, Protein-inorganic hybrid nanoflowers, Nat. Nanotechnol. 7 (2012) 428–432.
[102] L. Duan, H. Li, Y. Zhang, Synthesis of hybrid nanoflower-based carbonic anhydrase for enhanced biocatalytic activity and stability, ACS Omega 3 (2018) 18234–18241.
[103] S.W. Lee, S.A. Cheon, M. Kim II, T.J. Park, Organic-inorganic hybrid nanoflowers: types, characteristics, and future prospects, J. Nanobiotechnol. 13 (2015) 54.
[104] M.G. Lionetto, R. Caricato, M.E. Giordano, T. Schettino, The complex relationship between metals and carbonic anhydrase: new insights and perspectives, Int. J. Mol. Sci. 17 (2016).
[105] W.L. Nettles, H. Song, E.R. Farquhar, N.C. Fitzkee, J.P. Emerson, Characterization of the Copper(II) binding sites in human carbonic anhydrase II, Inorg. Chem. 54 (2015) 5671–5680.
[106] V.M. Krishnamurthy, et al., Carbonic anhydrase as a model for biophysical and physical-organic studies of proteins and protein-ligand binding, Chem. Rev. 108 (2008) 946–1051.
[107] H. Wen, et al., Bimetal based inorganic-carbonic anhydrase hybrid hydrogel membrane for CO_2 capture, J. CO2 Util. 39 (2020) 101171.
[108] Y. Li, et al., The influence of synthesis conditions on enzymatic activity of enzyme-inorganic hybrid nanoflowers, J. Mol. Catal. B Enzym. 133 (2016) 92–97.
[109] M. Oviya, V. Sukumaran, S.S. Giri, Immobilization and characterization of carbonic anhydrase purified from E. coli MO1 and its influence on CO_2 sequestration, World J. Microbiol. Biotechnol. 29 (2013) 1813–1820.
[110] A. Rohatgi, WebPlotDigitizer User Manual Version 3.4, URL http//arohatgi.info/WebPlotDigitizer/app, 2015, pp. 1–18, https://doi.org/10.5281/zenodo.10532.
[111] S. Hatta, No title, Technol. Rep. Töhoku Univ. 8 (1928).
[112] S. Zhang, Y. Lu, Kinetic performance of CO2 absorption into a potassium carbonate solution promoted with the enzyme carbonic anhydrase: comparison with a monoethanolamine solution, Chem. Eng. J. 279 (2015) 335–343.
[113] P. Usubharatana, P. Tontiwachwuthikul, Enhancement factor and kinetics of CO_2 capture by MEA-methanol hybrid solvents, Energy Procedia 1 (2009) 95–102. Elsevier.
[114] C. Ye, G. Chen, Q. Yuan, Process characteristics of CO_2 absorption by aqueous monoethanolamine in a microchannel reactor, Chin. J. Chem. Eng. 20 (2012) 111–119.
[115] C.A. Scholes, M. Simioni, A. Qader, G.W. Stevens, S.E. Kentish, Membrane gas-solvent contactor trials of CO_2 absorption from syngas, Chem. Eng. J. 195–196 (2012) 188–197.
[116] J.K.J. Yong, G.W. Stevens, F. Caruso, S.E. Kentish, In situ layer-by-layer assembled carbonic anhydrase-coated hollow fiber membrane contactor for rapid CO_2 absorption, J. Memb. Sci. 514 (2016) 556–565.
[117] A.H.G. Cents, D.W.F. Brilman, G.F. Versteeg, CO_2 absorption in carbonate/bicarbonate solutions: the Danckwerts-criterion revisited, Chem. Eng. Sci. 60 (2005) 5830–5835.
[118] A. Gladis, N.F. Lomholdt, P.L. Fosbøl, J.M. Woodley, N. von Solms, Pilot scale absorption experiments with carbonic anhydrase-enhanced MDEA- benchmarking with 30 wt% MEA, Int. J. Greenh. Gas Control 82 (2019) 69–85.
[119] X. Ye, Y. Lu, CO2 absorption into catalyzed potassium carbonate-bicarbonate solutions: kinetics and stability of the enzyme carbonic anhydrase as a biocatalyst, Chem. Eng. Sci. 116 (2014) 567–575.
[120] Fradette, S., Gingras, J., Carley, J., Kelly, G. R. & Ceperkovic, O. Process for capturing CO_2 from a gas using carbonic anhydrase and potassium carbonate. U.S. Pat. No. 9,533,258 (2017).
[121] I. Iliuta, M.C. Iliuta, Enzymatic CO_2 capture in countercurrent packed-bed column reactors with high performance random packings, Int. J. Greenh. Gas Control 63 (2017) 462–474.
[122] M. Leimbrink, T. Limberg, A.K. Kunze, M. Skiborowski, Different strategies for accelerated CO_2 absorption in packed columns by application of the biocatalyst carbonic anhydrase, Energy Procedia 114 (2017) 781–794.
[123] M. Leimbrink, et al., Pilot scale testing and modeling of enzymatic reactive absorption in packed columns for CO_2 capture, Int. J. Greenh. Gas Control 62 (2017) 100–112.
[124] F. Migliardini, et al., Biomimetic CO_2 capture using a highly thermostable bacterial α-carbonic anhydrase immobilized on a polyurethane foam, J. Enzyme Inhib. Med. Chem. 29 (2014) 146–150.
[125] S. Bhattacharya, A. Nayak, M. Schiavone, S.K. Bhattacharya, Solubilization and concentration of carbon dioxide: novel spray reactors with immobilized carbonic anhydrase, Biotechnol. Bioeng. 86 (2004) 37–46.
[126] M.E. Russo, et al., Post-combustion carbon capture mediated by carbonic anhydrase, Sep. Purif. Technol. 107 (2013) 331–339.

[127] M.E. Russo, et al., Modeling of slurry staged bubble column for biomimetic CO_2 capture, Int. J. Greenh. Gas Control 47 (2016) 200–209.
[128] M. Leimbrink, et al., Enzymatic reactive absorption of CO2 in MDEA by means of an innovative biocatalyst delivery system, Chem. Eng. J. 334 (2018) 1195–1205.
[129] I. Iliuta, M.C. Iliuta, Enhanced enzyme-based CO_2 capture in countercurrent packed-bed column reactors, Sep. Purif. Technol. 116908 (2020), https://doi.org/10.1016/j.seppur.2020.116908.
[130] Fradette, S., Gingras, J., Carley, J., Kelly, G. R. & Ceperkovic, O. Process for CO2 capture using carbonates and biocatalysts with absorption of CO2 and desorption of ion-rich solution. U.S. Pat. No. 8,722,391 (2014).
[131] Fradette, S. et al. Process for CO2 capture using micro-particles comprising biocatalysts. U.S. Pat. No. 8,846,377 (2014).
[132] G.F. Versteeg, S. Fradette, C02 Treatments Using Enzymatic Particles Sized According to Reactive Liquid Film Thickness for Enhanced Catalysis, Int. Publ. Number WO 2012/103653 Al, 2012.
[133] Penders, N. J. M.., Derks, P. W. J., Versteeg, G. F. & Fradette, S. Enzyme enhanced CO_2 capture and desorption processes. U.S. Pat. Appl. No. 13/503,808 (2013).
[134] Blais, R. & Rogers, P. Process and apparatus for the treatment of carbon dioxide with carbonic anhydrase. U.S. Pat. No. 6,524,843 (2003).
[135] E. Madore, S. Fradette, J. Lawson, Activity Replenishment and in Situ Activation for Enzymatic CO_2 Capture Packed Reactor, US20150104782 A1 (2012).
[136] T.L. Bucholz, et al., Development of an organosilica coating containing carbonic anhydrase for applications in CO2 capture. Novel Materials for Carbon Dioxide Mitigation Technology, Elsevier, 2015, pp. 117–147, https://doi.org/10.1016/b978-0-444-63259-3.00004-5.
[137] Fradette, S. Process and apparatus using a spray absorber bioreactor for the biocatalytic treatment of gases. Pat. number WO2004056455A1 (2004).
[138] Parent, C. & Dutil, F. Triphasic process for gas effluent treatment. U.S. Pat. No. 7,579,185. (2007).
[139] Verma, M., Fradette, L., Fradette, S., Lefebvre, S. & Sylvestre-Laurence, V. Intensification of biocatalytic gas absorption. US20180280871 (2018).
[140] C.R. Thomas, D. Geer, Effects of shear on proteins in solution, Biotechnol. Lett. 33 (2011) 443–456.
[141] T.P. Gunjikar, S.B. Sawant, J.B. Joshi, Shear deactivation of cellulase, exoglucanase, endoglucanase, and β-glucosidase in a mechanically agitated reactor, Biotechnol. Prog. 17 (2001) 1166–1168.
[142] J.L. Li, B.H. Chen, Review of CO_2 absorption using chemical solvents in hollow fiber membrane contactors, Sep. Purif. Technol. 41 (2005) 109–122.
[143] P. Luis, B. Van der Bruggen, T. Van Gerven, Non-dispersive absorption for CO_2 capture: from the laboratory to industry, J. Chem. Technol. Biotechnol. 86 (2011) 769–775.
[144] J.L. Kaar, H. Oh II, A.J. Russe II, W.J. Federspiel, Towards improved artificial lungs through biocatalysis, Biomaterials 28 (2007) 3131–3139.
[145] D.T. Arazawa, et al., Immobilized carbonic anhydrase on hollow fiber membranes accelerates CO2 removal from blood, J. Memb. Sci. 403–404 (2012) 25–31.
[146] J.D. Kimmel, et al., Carbonic anhydrase immobilized on hollow fiber membranes using glutaraldehyde activated chitosan for artificial lung applications, J. Mater. Sci. Mater. Med. 24 (2013) 2611–2621.
[147] D.T. Arazawa, J.D. Kimmel, M.C. Finn, W.J. Federspiel, Acidic sweep gas with carbonic anhydrase coated hollow fiber membranes synergistically accelerates CO_2 removal from blood, Acta Biomater. 25 (2015) 143–149.
[148] D.T. Arazawa, J.D. Kimmel, W.J. Federspiel, Kinetics of CO_2 exchange with carbonic anhydrase immobilized on fiber membranes in artificial lungs, J. Mater. Sci. Mater. Med. 26 (2015).
[149] J.K.J. Yong, G.W. Stevens, F. Caruso, S.E. Kentish, The resilience of carbonic anhydrase enzyme for membrane-based carbon capture applications, Int. J. Greenh. Gas Control 62 (2017) 122–129.
[150] Y. Xu, Y. Lin, N.G.P. Chew, C. Malde, R. Wang, Biocatalytic PVDF composite hollow fiber membranes for CO_2 removal in gas-liquid membrane contactor, J. Memb. Sci. 572 (2019) 532–544.
[151] J. Hou, et al., Biocatalytic Janus membranes for CO_2 removal utilizing carbonic anhydrase, J. Mater. Chem. A 3 (2015) 17032–17041.
[152] J. Hou, et al., Biocatalytic gas-liquid membrane contactors for CO_2 hydration with immobilized carbonic anhydrase, J. Memb. Sci. 520 (2016) 303–313.
[153] I. Iliuta, M.C. Iliuta, Investigation of CO_2 removal by immobilized carbonic anhydrase enzyme in a hollow-fiber membrane bioreactor, AIChE J. 63 (2017) 2996–3007.
[154] Stolaroff, J. K. et al. Bioreactors including enzyme - embedded multicomponent polymers. U.S. Pat. No. 10,202,567 (2019).
[155] J.G. Wijmans, R.W. Baker, The solution-diffusion model: a review, J. Memb. Sci. 107 (1995) 1–21.
[156] L. Zhao, E. Riensche, R. Menzer, L. Blum, D. Stolten, A parametric study of CO2/N2 gas separation membrane processes for post-combustion capture, J. Memb. Sci. 325 (2008) 284–294.
[157] L.M. Robeson, Correlation of separation factor versus permeability for polymeric membranes, J. Memb. Sci. 62 (1991) 165–185.
[158] R. Bounaceur, N. Lape, D. Roizard, C. Vallieres, E. Favre, Membrane processes for post-combustion carbon dioxide capture: a parametric study, Energy 31 (2006) 2556–2570.
[159] T.C. Merkel, H. Lin, X. Wei, R. Baker, Power plant post-combustion carbon dioxide capture: an opportunity for membranes, J. Memb. Sci. 359 (2010) 126–139.
[160] P. Luis, T. Van Gerven, B. Van Der Bruggen, Recent developments in membrane-based technologies for CO_2 capture, Prog. Energy Combust. Sci. 38 (2012) 419–448.
[161] W.J. Ward, W.L. Robb, Carbon dioxide-oxygen separation: facilitated transport of carbon dioxide across a liquid film, Science 156 (1967) 1481–1484.
[162] S.R. Suchdeo, J.S. Schultz, Mass transfer of CO_2 across membranes: facilitation in the presence of bicarbonate ion and the enzyme carbonic anhydrase, BBA - Biomembr. 352 (1974) 412–440.
[163] Y. Fu, et al., Ultra-thin enzymatic liquid membrane for CO_2 separation and capture, Nat. Commun. 9 (2018).
[164] Jiang, Y. B., Cecchi, J. L., Rempe, S., Fu, Y., & Brinker, C. J. ENZYMATICALLY Active high-flux selectively gas-permeable membranes. (2016). doi:US Patent 9,242,210.
[165] L.A. Neves, C. Afonso, I.M. Coelhoso, J.G. Crespo, Integrated CO2capture and enzymatic bioconversion in supported ionic liquid membranes, Sep. Purif. Technol. 97 (2012) 34–41.
[166] A. Bednár, et al., Enzymatically-boosted ionic liquid gas separation membranes using carbonic anhydrase of biomass origin, Chem. Eng. J. 303 (2016) 621–626.
[167] M.Y. Abdelrahim, et al., Supported ionic liquid membranes immobilized with carbonic anhydrases for CO_2 transport at high temperatures, J. Memb. Sci. 528 (2017) 225–230.
[168] N. Nemestóthy, P. Bakonyi, Z. Németh, K. Bélafi-Bakó, Evaluation of pectin-reinforced supported liquid membranes containing carbonic anhydrase: the role of ionic liquid on enzyme stability and CO_2 separation performance, J. CO2 Util. 24 (2018) 59–63.
[169] R. Craveiro, L.A. Neves, A.R.C. Duarte, A. Paiva, Supported liquid membranes based on deep eutectic solvents for gas separation processes, Sep. Purif. Technol. 254 (2021) 117593.
[170] A.M. de Castro, et al., Role of water on deep eutectic solvents (DES) properties and gas transport performance in biocatalytic supported DES membranes, Sep. Purif. Technol. 255 (2021) 117763.
[171] L.J. Lozano, et al., Recent advances in supported ionic liquid membrane technology, J. Memb. Sci. 376 (2011) 1–14.
[172] J. Ge, R.M. Cowan, C. Tu, M.L. McGregor, M.C. Trachtenberg, Enzyme-based CO2 capture for advanced life support, Life Support Biosph. Sci. 8 (2002) 181–189.
[173] R.M. Cowan, J. Ge, Y. Qin, M.L.M.C. Gregor, CO 2 capture by means of an enzyme-based reactor, Ann. N. Y. Acad. Sci. 984 (2003) 453–469.
[174] S. Duan, T. Kai, S.I. Nakao, Effect of carbonic anhydrase on CO_2 separation performance of thin poly(Amidoamine) dendrimer/poly(ethylene glycol) hybrid membranes, Membranes 9 (2019) 167.
[175] L. Bao, M.C. Trachtenberg, Facilitated transport of CO_2 across a liquid membrane: comparing enzyme, amine, and alkaline, J. Memb. Sci. 280 (2006) 330–334.
[176] Y.T. Zhang, L. Zhang, H.L. Chen, H.M. Zhang, Selective separation of low concentration CO_2 using hydrogel immobilized CA enzyme based hollow fiber membrane reactors, Chem. Eng. Sci. 65 (2010) 3199–3207.
[177] L.H. Cheng, L. Zhang, H.L. Chen, C.J. Gao, Hollow fiber contained hydrogel-CA membrane contactor for carbon dioxide removal from the enclosed spaces, J. Memb. Sci. 324 (2008) 33–43.
[178] Y. Zhang, H. Wang, J. Liu, J. Hou, Y. Zhang, Enzyme-embedded metal-organic framework membranes on polymeric substrates for efficient CO_2 capture, J. Mater. Chem. A 5 (2017) 19954–19962.
[179] Sandru, M., Sandru, E. M. & Stenstad, P. M. Hybrid polymer. Int. Publ. Number WO 2019/212359A2 (2019).
[180] S. Ren, S. Jiang, X. Yan, R. Chen, H. Cui, Challenges and opportunities: porous supports in carbonic anhydrase immobilization, J. CO2 Util. 42 (2020) 101305.
[181] Z. Wu, et al., Immobilization of carbonic anhydrase for facilitated CO_2 capture and separation, Chin. J. Chem. Eng. (2020), https://doi.org/10.1016/j.cjche.2020.06.002.
[182] A. Nuchitprasittichai, S. Cremaschi, Sensitivity of amine-based CO_2 capture cost: the influences of CO2 concentration in flue gas and utility cost fluctuations, Int. J. Greenh. Gas Control 13 (2013) 34–43.
[183] R. Barbero, et al., Engineered yeast for enhanced CO_2 mineralization, Energy Environ. Sci. 6 (2013) 660–674.
[184] S.S.W. Effendi, I.S. Ng, The prospective and potential of carbonic anhydrase for carbon dioxide sequestration: a critical review, Process Biochem. 87 (2019) 55–65.
[185] A.L. Demain, P. Vaishnav, Production of recombinant proteins by microbes and higher organisms, Biotechnol. Adv. 27 (2009) 297–306.
[186] P. Tufvesson, J. Lima-Ramos, M. Nordblad, J.M. Woodley, Guidelines and cost analysis for catalyst production in biocatalytic processes, Org. Process Res. Dev. 15 (2011) 266–274.
[187] D. Klein-Marcuschamer, P. Oleskowicz-Popiel, B.A. Simmons, H.W. Blanch, The challenge of enzyme cost in the production of lignocellulosic biofuels, Biotechnol. Bioeng. 109 (2012) 1083–1087.
[188] J.B. Beilen, Z. Li, Enzyme technology: an overview, Curr. Opin. Biotechnol. 13 (2002) 338–344.
[189] S. Gilassi, S.M. Taghavi, D. Rodrigue, S. Kaliaguine, Techno-economic evaluation of membrane and enzymatic-absorption processes for CO_2 capture from flue-gas, Sep. Purif. Technol. 248 (2020).
[190] A. Di Fiore, V. Alterio, S.M. Monti, G. De Simone, K. D'Ambrosio, Thermostable carbonic anhydrases in biotechnological applications, Int. J. Mol. Sci. 16 (2015) 15456–15480.

[191] F. Saunier, et al., Comparison of life-cycle assessment between bio-catalyzed and promoted potassium carbonate processes and amine-based carbon capture technologies, Int. J. Greenh. Gas Control 88 (2019) 134–155.
[192] S. Zhang, H. Lu, Y. Lu, Enhanced stability and chemical resistance of a new nanoscale biocatalyst for accelerating CO_2 absorption into a carbonate solution, Environ. Sci. Technol. 47 (2013) 13882–13888.
[193] J.K.J. Yong, G.W. Stevens, F. Caruso, S.E. Kentish, The use of carbonic anhydrase to accelerate carbon dioxide capture processes, J. Chem. Technol. Biotechnol. 90 (2015) 3–10.